Carbon budgets of Scotia Sea mesopelagic zooplankton and micronekton communities during austral spring

Kathryn B. Cook [a,f,*], Anna Belcher [b], Daniel Bondyale Juez [c], Gabriele Stowasser [b],
Sophie Fielding [b], Ryan A. Saunders [b], Mohamed A. Elsafi [d], George A. Wolff [e],
Sabena J. Blackbird [e], Geraint A. Tarling [b], Daniel J. Mayor [a,f]

[a] National Oceanography Centre, Southampton, SO14 3ZH, UK
[b] British Antarctic Survey, Cambridge, CB3 0ET, UK
[c] EOMAR, Universidad de Las Palmas de Gran Canaria, Spain
[d] Oceanography Department, Faculty of Science, Alexandria University, Egypt
[e] School of Environmental Sciences, University of Liverpool, Liverpool, L69 3GP, UK
[f] Department of Biosciences, University of Exeter, Exeter, EX4 4PS, UK

ARTICLE INFO

ABSTRACT

Zooplankton form an integral component of epi- and mesopelagic ecosystems, and there is a need to better understand their role in ocean biogeochemistry. The export and remineralisation of particulate organic matter at depth plays an important role in controlling atmospheric CO_2 concentrations. Pelagic mesozooplankton and micronekton communities may influence the fate of organic matter in a number of ways, including: the consumption of primary producers and export of this material as fast-sinking faecal pellets, and the active flux of carbon by animals undertaking diel vertical migration (DVM) into the mesopelagic. We present day and night vertical biomass profiles of mesozooplankton and micronekton communities in the upper 500 m during three visits to an ocean observatory station (P3) to the NW of South Georgia (Scotia Sea, South Atlantic) in austral spring, alongside estimates of their daily rates of ingestion and respiration throughout the water column. Day and night community biomass estimates were dominated by copepods >330 μm, including the lipid-rich species, *Calanoides acutus* and *Rhincalanus gigas*. We found little evidence of synchronised DVM, with only *Metridia* spp. and *Salpa thompsoni* showing patterns consistent with migratory behaviour. At depths below 250 m, estimated community carbon ingestion rates exceeded those of metabolic costs, supporting the understanding that food quality in the mesopelagic is relatively poor, and organisms have to consume a large amount of food in order to fulfil their nutritional requirements. By contrast, estimated community rates of ingestion and metabolic costs at shallower depths were approximately balanced, but only when we assumed that the animals were predominantly catabolising lipids (i.e. respiratory quotient = 0.7) and had relatively high absorption efficiencies. Our work demonstrates that it is possible to balance the metabolic budgets of mesopelagic animals to within observational uncertainties, but highlights the need for a better understanding of the physiology of lipid-storing animals and how it influences carbon budgeting in the pelagic.

1. Introduction

The photosynthetic production of organic matter in the surface ocean, and its subsequent export and remineralisation at depth, plays a fundamental role in controlling atmospheric CO_2 levels (Boyd et al., 2019). The depth at which sinking organic particles are consumed and respired by midwater organisms influences the timeframe over which

the constituent carbon is isolated from the atmosphere and hence 'sequestered' (Kwon et al., 2009). Quantifying and understanding the myriad processes that make up the ocean's 'biological gravitational pump' (BGP), and how it will respond to future climate, remain major goals of contemporary biological oceanography.

The majority of sinking particulate organic matter (POM) that leaves the base of the euphotic zone is remineralised within the mesopelagic

---

zone, which extends down to 1000 m (Buesseler et al., 2007; Steinberg et al., 2008; Giering et al., 2014). The collective respiratory demands of organisms within this zone should, at steady state, equal the removal of sinking carbon flux. However, until recently, attempts to compare the biological requirements for organic carbon with that supplied have produced considerable mismatches, with the former exceeding the latter by up to two orders of magnitude (reviewed by Burd et al., 2010). In 2014, the first balanced mesopelagic carbon budget was published for the long-term monitoring site at the Porcupine Abyssal Plain, NE Atlantic (Giering et al., 2014), highlighting the importance of mesopelagic animals and their interactions with sinking particles. Zooplankton and micronekton communities contribute to, and interact with, the BGP passively *via* the production of sinking particles such as faecal pellets and carcasses, and actively *via* feeding on sinking particles and through diel vertical migrations (DVM) which remove carbon from surface waters and transport it to below the euphotic zone (See reviews by Steinberg and Landry, 2017; Le Moigne, 2019).

Zooplankton and micronekton feeding in the epipelagic re-package slow-sinking organic matter into dense, faster sinking faecal pellets that increase the gravitational flux of carbon (Turner, 2015). The magnitude of particle flux and sinking speeds varies with pelagic community biomass, composition, grazing rates and behaviour (Zøllner et al., 2009; Manno et al., 2015; Belcher et al., 2016, 2019a; Polimene et al., 2017; Liszka et al., 2019; Yang et al., 2019). Particle sinking speeds, including those of faecal pellets, can be modified through fragmentation (Briggs et al., 2020). Indeed, particle fragmentation by the feeding activities of zooplankton resident in the mesopelagic has been suggested to arrest a significant fraction of the sinking flux and may therefore influence how deep particles penetrate into the ocean's interior (Mayor et al., 2014, 2020).

DVM of zooplankton and micronekton, where animals reside at depth during the day and migrate to feed at the surface at night, is widely reported in marine ecosystems (reviewed by Bandara et al., 2021). These migrations actively transport carbon ingested in the epipelagic to the mesopelagic where it may be released via excretion, respiration, egestion and mortality at depth (Steinberg and Landry, 2017 and references therein), and so are often incorporated into biogeochemical models (e.g. Longhurst et al., 1990; Hansen and Visser, 2016; Archibald et al., 2019; Kelly et al., 2019). Mesopelagic micronekton can generate a significant proportion of total respiratory fluxes (e.g. Hidaka et al., 2001; Ariza et al., 2015; Belcher et al., 2019b), but direct measurements from the mesopelagic are limited as it is difficult to collect animals for incubation measurements without damaging them, and it is also hard to replicate the changing temperature and pressure conditions experienced *in situ* during migration. Mesopelagic organisms can therefore play an important role in the biological carbon pump, yet quantifying how they affect the numerous carbon flow pathways that they are involved in remains challenging.

The COMICS (Controls over Ocean Mesopelagic Interior Carbon Storage) programme was designed to deliver new insights into the processes influencing carbon cycling in the mesopelagic zone and hence the storage of carbon in the ocean (Sanders et al., 2016). Quantifying the vertical distribution and movements of zooplankton, along with their feeding behaviours and metabolic requirements, is integral to understanding how ocean biology contributes to this process. The region downstream from South Georgia in the Scotia Sea, South Atlantic, is an iron-fertilised hotspot of productivity that supports an extensive phytoplankton bloom and high biomass of mesozooplankton and micronekton (Korb et al., 2012; Ward et al., 2012), resulting in high levels of carbon export to the deep ocean. Station P3, a long-term mooring observatory (Scotia Sea open-ocean biological programme of Sustained Observation, British Antarctic Survey, NERC; Manno et al., 2015) in this region, which forms part of a programme of sustained observations in the open-ocean Scotia Sea, was chosen as the site for COMICS fieldwork (Sanders et al., 2016). Day and night depth profiles of mesozooplankton and micronekton biomass were collected to estimate

the magnitude of DVM. The respiration rates of mesozooplankton and micronekton communities were determined using a combination of Electron Transport System (ETS) and biomass measurements combined with allometric calculations. Grazing experiments were also conducted for resident and potentially migratory mesopelagic mesozooplankton species. These data were used to generate carbon budgets of the mesopelagic zooplankton and micronekton communities in the Scotia Sea.

2. Methods

Sampling for this study was conducted during a research cruise to the Scotia Sea in the Southern Ocean in austral spring (DY086; November 12, 2017–December 19, 2017) aboard the *RRS Discovery* (cruise report: Giering et al., 2019a). Sampling was focused at station P3, a long-term observation site (Tarling et al., 2012; Manno et al., 2015, 2022), located to the northwest of South Georgia (52.40 °S, 40.06°W). The same station was occupied on three occasions, defined as stations P3A (15 - 22nd November), P3B (29th November – 5th December) and P3C (9–15th December). Vertical profiles of temperature were obtained from Conductivity-Temperature-Depth (CTD) unit (SBE 9 plus) deployments. Daylight hours and lunar phase for each sampling date were taken from SunriseSunset.com for the latitude and longitude of P3.

2.1. Mesozooplankton and micronekton

2.1.1. Net sampling

To effectively sample across the size range of organisms (0.1 mm–300 mm) encompassed by the classifications of mesozooplankton to micronekton, we required a multi-net-sampling strategy (Table 1) as a result of differing sampling efficiencies (Wiebe and Benfield, 2003). A Hydrobios Mammoth Net (hauled at 0.2 ms^{-1}) and a motion-compensated opening/closing Bongo net (hauled at 0.3 ms^{-1}) were deployed vertically to sample mesozooplankton. The Bongo was generally set out in two sequential deployments with one sampling the top 150 m, and the other sampling from 150m to 500 m. Mammoth deployments were repeated day and night, but Bongo deployments for biomass measurements only took place during the day. Additional Bongo deployments at the same depths were made in order to collect live animals for grazing experiments. The water volumes filtered by the Bongo and Mammoth nets were calculated using the net dimensions and depth of water sampled assuming 100% efficiency (Ward et al., 2012).

To collect the larger mesozooplankton and micronekton, we deployed a MOCNESS (Multiple Opening and Closing Nets and Environmental Sampling System, Wiebe and Benfield, 2003) and an RMT25 (opening and closing 25 m^2 rectangular mid-water trawl net, Baker et al., 1973; Piatkowski et al., 1994). Both nets were towed obliquely at a speed of 2 knots, and deployments were repeated day and night. The MOCNESS was towed for 10 min in each depth layer, and the volume filtered was calculated using a flow meter and estimated effective mouth area. The RMT was towed for 40 min in each depth layer, and the volume filtered was calculated using the net dimensions and the distance travelled by the net.

2.2. Sample handling and biomass measurements

2.2.1. Biomass

One net of the Bongo catches was preserved in 4% borax buffered formaldehyde for particle enumeration using a FlowCam Macro (Yokogawa Fluid Imaging Technologies Inc.). One set of preserved Bongo samples was also sent to the NMFRI Plankton Sorting and Identification Centre, Poland, for species identification and enumeration.

MOCNESS catches were split into two aliquots, using a Folsom plankton splitter, with one half being preserved in 4% borax buffered formaldehyde for biomass analysis. These were sent to the NMFRI Plankton Sorting and Identification Centre, Poland, for species identification and enumeration of subsamples containing at least 500

Table 1
Summary of multi-net sampling strategy. Bongo nets were only deployed during the day, all other net deployments were repeated day and night.

Sampler	Target group	Mesh size (mm)	Mouth area (m^2)	Net depth strata (m)	Analysis
Bongo (n = 16)	Small mesozooplankton: microcopepods, small calanoid copepods	0.1	0.29	0–150 150–500	- Abundance: FlowCam Macro - Biomass: Abundance × mass (Table S2) - Community respiration: Whole sample ETS - Copepod grazing (Table 2) - Community ingestion: Biomass × daily ration (Table S7)
Bongo (n = 1)	Small mesozooplankton: microcopepods, small calanoid copepods	0.1	0.29	0–75 75–150 150–250 250–500	- Biomass specific respiration: Whole sample ETS
Mammoth (n = 4)	Mesozooplankton: large calanoid copepods, larval euphausiids	0.3	1	0–33 33–63 63–125 125–188 188–250 250–313 313–375 375–438 438–500	- Biomass specific respiration: Whole sample ETS
MOCNESS (n = 4)	Large mesozooplankton and small micronekton: fast swimming small euphausiids, chaetognaths, salps	0.33	1	0–62 62–125 125–187 187–250 250–312 312–375 375–437 437–500	- Abundance: Manual - Biomass: Abundance × mass (Ward et al., 2012) - Community respiration: Biomass × specific respiration - Community ingestion: Biomass × daily ration (Table S7)
RMT25 (n = 6)	Micronekton: Krill, mesopelagic fish, cephalopods, large cnidarians	4	25	0–250 250–500	- Wet weight (WW) - Biomass: WW:Dry Mass (DM; Tables S5 and S6) - Community respiration: Individual ETS (Fish, euphausiids); WW to respiration (Table S3); DM to respiration (Table S4) - Community ingestion: Biomass × daily ration (Table S7)

Table 2
Summary of copepod grazing experiments.

Species	Station	Stage	No. animals	Incubation vol (L)	Water collection depth (m)	Average % cells remaining
Oithona similis (applied to cyclopoid and harpacticoid copepods)	P3A	CV-CVI	20	0.2	20	80
		CV-CVI	20	0.2	350	89
	P3B	CIII-IV	20	0.2	30	80
	P3C	CV-CVI	20	0.2	75	88
		CIII-IV	30	0.2	75	86
Calanoides acutus (applied to *Calanus* spp.)	P3A	CIV-CV	5	1.1	30	94
	P3B	CV	7	1.1	30	94
	P3C	CV	5	1.1	30	79
Rhincalanus gigas	P3A	CVI	1	1.1	30	88
	P3B	CVI	1	1.1	30	95
	P3C	CVI	1	1.1	30	85
Ctenocalanus spp. (applied to small calanoid copepods)	P3A	CV-CVI	20	1.1	30	87
Metridia spp. (applied to Metridinidae and Euchaetidae)	P3B	CVI	8	1.1	30	80

individuals, and the data were used to calculate biomass by applying a published mass factor to each taxonomic entity (Ward et al., 2012). For euphausiids sampled by the MOCNESS net (all except *Euphausia superba* where composite weight was measured from the RMT25) we estimated the biomass of the enumerated species using literature-derived estimates of wet mass (WM). For *Thysanoessa* spp. we estimated a representative WM of 46.6 mg using a length of 20 mm taken from Siegel (1987) and the length-weight relationship of Siegel (1992). For the remaining euphausiid species (of which *Euphausia frigida* was the dominant species), we estimated a representative WM of 34.5 mg using a mean length of 18 mm (Kittel et al., 1985; Siegel, 1987) and the relationship of Siegel (1992). The second MOCNESS aliquot was used to collect animals for

other analyses including lipid content. Replicate samples of two C6 female *Rhincalanus gigas* or five C5 *Calanoides acutus* were rapidly picked into glass vials in a controlled temperature laboratory set at the *in situ* surface temperature (2 °C) and immediately stored at −80 °C.

RMT25 catches were analysed immediately to determine taxonomic composition, abundance and WM of the whole sample. Fish were identified and weighed individually, whilst other taxa were counted and weighed in batches. The mean individual WM of micronekton species from the RMT25 net was calculated using the total abundance and total WM for each species.

Weighted Mean Depth (WMD) of total biomass and selected taxa from the MOCNESS and RMT nets were calculated using equation (1):

$$\text{WMD (m)} = \sum (b_i \times d_i) \Big/ B \qquad \text{(eq 1)}$$

Where b_i is the biomass (mg C m^{-3}) in net i, d_i is the mid-depth (m) of net i, and B is the biomass in all nets. Day WMD was subtracted from night WMD to determine the depth change due to diel migration (ΔWMD).

2.2.2. FlowCam macro

The preserved Bongo samples were sub-sampled using a Folsom splitter where necessary, such that a minimum of 2000 particles were counted. Images were collected using a 5 mm flow cell, a flow rate of 700 mL min^{-1} and an auto-image mode rate of 10 frames per second. Images were classified manually into broad taxonomic groups (cyclopoid copepods, small calanoid copepods, large calanoid copepods, *Rhincalanus gigas*, *Metridia* spp., polychaetes, gastropods, ostracods, appendicularians, euphausiids) to determine abundance using Visual-Spreadsheet software (Version 4.3.55). These data were used to calculate biomass by applying mass factors (Ward et al., 2012) to the abundance of each taxonomic entity (see Supplementary Table S1). Mass factors were calculated from published values (Ward et al., 2012) weighted by the relative abundance of the species within a taxonomic entity found in the Bongo net samples that were sent for taxonomic analysis. This had the effect of placing more emphasis on the taxa that dominated in the respective broad taxonomic groups.

2.2.3. Metabolic rates

One net of the Bongo catches was size fractionated (100–200 μm, 200–500 μm, 500–1000 μm, 1000–2000 μm, >2000 μm) and frozen at −80 °C for later measurement of Electron Transport System (ETS) activity (Owens and King, 1975). During one station (P3C), a set of Bongo net samples taken from 0 to 75m, 75–150m, 150–250m and 250–500m were frozen, without size fractionation, for measurement of the ETS activity of the total community. Separate Bongo deployments collected animals for grazing experiments, which were diluted in fresh seawater and immediately moved to a controlled temperature laboratory set to *in situ* surface temperature (2 °C).

Mammoth catches were frozen at −80 °C for later measurement of ETS activity of the >300 μm mesozooplankton community. A subsample of the dominant taxa found in the RMT catch was immediately flash frozen in liquid nitrogen and stored at −80 °C for later measurement of ETS activity. 10-40 replicate ETS samples were taken for each taxa.

2.3. Acoustic sampling

A multi-frequency (18, 38, 70, 120 and 200 kHz) drop-keel mounted echosounder (Simrad EK60) collected acoustic backscattering data (S$_v$, dB re 1 m^{-1}) throughout the cruise, where acoustic backscatter is used as a proxy for mesozooplankton and micronekton biomass (depending on frequency). The echosounder was calibrated using standard sphere techniques (Demer et al., 2015) in Stromness Harbour, South Georgia on 27/11/2017. Raw data were collected to 1500 m at a ping rate of 3 s. Frequency specific mean values of sound speed (Mackenzie, 1981) and absorption coefficient (Francois and Garrison, 1982) were derived from CTD profiles for the typical depth ranges ensonified by each frequency, limited by the maximum depth of data used here (1000m, 1000m, 750m, 500m, 250m (18, 38, 70, 120 and 200 kHz respectively)). Data were processed in Echoview V10 (10.0.293.38183), this included: updating values of sound speed and absorption; cleaning noise (transient (set to −999 dB), intermittent (set to −999 dB) and background noise removed); removing periods when the vessel was on station (ship speed <2 knots); and resampling to then export S$_v$ (dB re 1 m^{-1}) in cells of 1m vertical resolution and 10 min horizontal. These data were allocated to day or night categories and further averaged to generate profiles of day and night distribution.

2.4. Respiration

2.4.1. Electron transport system (ETS) activity

To estimate respiration, we carried out ETS activity assays following the method of Owens and King (1975) with modifications from Gómez et al. (1996). Frozen specimens were reweighed in the laboratory. We used a weighed sub-sample, taken from just behind the head, for fish species caught by the RMT, whole individuals for other micronekton species, and the whole net sub-sample (split or size fraction) for mesozooplankton measurements. See Belcher et al. (2020) for further details about the specific mesopelagic fish respiration results.

Each sample was homogenised in a phosphate buffer, using either an electric homogeniser or a sonicator, for 30–60 s, before being centrifuged at 4000 rpm for 10 min at 0°C. 100 μL of the homogenate supernatant and 300 μL of reaction buffer (0.1 M, pH 8.5) containing substrates nicotinamide adenine dinucleotide (NADH) and nicotinamide adenine dinucleotide phosphate (NADPH) (saturating concentrations of 1.7 and 0.25 mM, respectively) were added to a semi-micro quartz cuvette. 100 μL 2-*p*-iodophenyl-3-*p*-nitrophenyl monotetrazolium chloride (INT, 4 mM) was added to each cuvette to commence the reaction. All procedures were carried out on ice. The reaction was measured continuously for 8 min at a wavelength of 490 nm in a Cary 60 UV–Vis spectrophotometer (Packard and Christensen, 2004). The temperature of the reaction was controlled at 12 °C. To take into account the non-enzymatic reduction of INT (Maldonado et al., 2012), a blank assay was also performed without ETS substrates for each sample. Reagent blanks were taken daily.

Formazan is produced during the kinetic assay as INT is reduced. INT takes the place of oxygen as the electron acceptor in the ETS, and accepts two electrons (oxygen would accept four). Therefore, the rate of formazan produced is related to oxygen consumption by a factor of two. Using the formazan production rate and our measured INT extinction coefficient (measured at 490 nm for each batch of INT; 13.3–16.4 mM^{-1} cm^{-1}) we calculated the potential respiration rate (Φ, μmol O$_2$ h^{-1}) following Packard and Christensen (2004). Using a conservative respiration to ETS (R:ETS) ratio of 0.5 (Ikeda, 1985; Hernández-León and Gómez, 1996), we then estimated the respiration at the experimental temperature of 12 °C. Where a subsample was taken (*i.e.* for fish), the total respiration rate per individual was calculated based on the ratio between the subsample and the total weight of the fish. To estimate the respiration rate at *in situ* temperatures, defined as the temperature from the CTD averaged over the net depth horizon, we used the Arrhenius equation and an activation energy of 62.8 kJ mol^{-1} (15 kcal mol^{-1}; Packard et al., 1975; Ariza et al., 2015; Hernández-León et al., 2019b). Respiration rates per hour were multiplied by 24 to give respiration rates per day, and a respiratory quotient of 0.9 was used to convert from oxygen to carbon (Ariza et al., 2015).

2.4.2. Mesozooplankton respiration

For the samples where we measured ETS activity, carbon specific respiration rates were calculated and applied to the biomass estimates from Bongo and MOCNESS samples described above and integrated over the volume filtered by the net to give daily respiration rates per m^3. WM of the ETS samples were converted to DM using a conversion factor of 0.25 (Kiørboe, 2013) and then to C using a conversion factor of 0.45 (Giering et al., 2019b). The carbon specific respiration (d^{-1}) of the equivalent Mammoth net was applied to the biomass from the MOCNESS net samples. For station P3B, where no Mammoth net ETS measurements were taken, the mean P3A and P3C specific respiration rates were applied. For the Bongo net, the carbon specific respiration (d^{-1}) of the appropriate size fraction was applied to each particle (based on area based diameter (ABD) measurements made by the FlowCam Macro) and summed for all particles in the Bongo sample.

2.4.3. Micronekton respiration

For the species where we measured ETS activity, we calculated

allometric regressions (see Supplementary Table S2) relating WM (mg) to ETS-derived respiration (μLO_2 Ind^{-1} h^{-1}), with equations in the form of equation (2) where a_o and a_1 are constants:

$$Ln\ (Respiration) = a_o + a_1 \times Ln\ (WM) \qquad (eq.\ 2)$$

We found no significant relationship between ETS-derived respiration and WM for *E. triacantha*, and thus we used the mean measured respiration rate of 13.925 μLO_2 Ind^{-1} h^{-1}.

It was not feasible to sample and conduct ETS assays on all species, thus we used allometric relationships from the literature to estimate respiration rates (μLO_2 Ind^{-1} h^{-1}) for those species we were not able to measure (See Belcher et al., 2020 for a comparison of ETS and allometrically derived respiration in these samples). Taking the data from, and following the form of the regressions given in, Ikeda (2014), (equation (3) below), we calculated taxa specific linear regressions using multiple predictors (dry mass (DM, mg), temperature (T) and habitat depth (z, m)) with no interaction terms, where a_o, a_1, a_2 and a_3 are constants. See Supplementary Table S3 for allometric equations.

$$Ln\ (Respiration) = a_0 + a_1 \times ln(DM) + a_2 \times 1000/T + a_3 \times ln(z) \qquad (eq.\ 3)$$

For cephalopods, we used the data of Ikeda (2016) and carried out the same procedure as above but using body mass as WM.

Where allometric equations required DM, we made appropriate conversions using a combination of our own measurements from the DY086 research cruise where possible (Supplementary Table S4) and conversions from the literature (Supplementary Table S5). Once respiration rates per individual had been calculated, we summed them for each net deployment, and integrated over the volume filtered by the net to give respiration rates m^{-3}. For the RMT25 we summed all but the small euphausiid species (all euphausiids excluding *E. superba*), and we added this to the summed respiration of small euphausiids from the MOCNESS to give the total micronekton respiration. Respiration rates per hour were multiplied by 24 to give respiration rates per day, and a respiratory quotient of 0.9 was used to convert from oxygen to carbon.

2.4.4. Total community respiration

Total community respiration was summed over the coarsest depth ranges that samples were taken from, i.e. 0–250m and 250–500m sampled by the RMT25. MOCNESS nets aligned readily into this range (nets 2-5 = 250–500m, nets 6-9 = 0–250m). Bongo net samples, however, were taken from 0 to 150m and 150–500m. Bongo respiration per m^3 in 250–500m was assumed to be the same as that for 150–500m. Bongo respiration in 0–250m (BR_{0-250}, $mmolC\ m^{-3}\ d^{-1}$) was calculated as a weighted mean of respiration rates for 0–150m (BR_{0-150}, $mmolC\ m^{-3}\ d^{-1}$) and 150–500m ($BR_{150-500}$, $mmolC\ m^{-3}\ d^{-1}$) (equation (4)). Only respiration for Bongo net particles less than 300 μm were included to avoid overlap with the MOCNESS respiration estimates.

$$BR_{0-250} = ((BR_{0-150}\ x\ 150) + (BR_{150-500}\ x\ 100))\ /\ 250 \qquad (eq.\ 4)$$

2.5. Ingestion

2.5.1. Copepod grazing experiments

All experimental work for grazing experiments was undertaken in a controlled temperature laboratory set at *in situ* surface temperature (2 °C). Experimental animals were collected using a motion-compensated Bongo net (100 μm mesh) using a non-filtering cod end (see section 2.1.1 above) and were sorted under dim light using a dissection microscope. Experimental water was collected using Niskin bottles attached to a CTD rosette or a Marine Snow Catcher (Riley et al., 2012). Incubations were carried out using water collected close to the subsurface chlorophyll maximum, and with water collected from additional depths for *Oithona similis*. Copepod grazing rates were examined using particle-removal experiments (Mayor et al., 2006). In brief, glass incubation bottles were filled with un-screened seawater a little at a time to maximise homogeneity. Visibly discernible copepods were removed

from the incubation bottle via a dip-tube. Experimental animals were carefully introduced into bottles and incubated in triplicate alongside triplicate control bottles in the dark on a plankton wheel rotating at 1 rpm for 24 h and were terminated by adding 1% acidified Lugol's iodine. Microplankton samples (200 mL) from the start of the experiment and from each of the incubated bottles were collected and preserved with acidified Lugol's iodine (1%). Experiments were conducted for dominant copepod species that represented different functional feeding types in the copepod community: small particle associated copepods (*Oithona similis*), small (*Ctenocalanus* spp.), intermediate (*Calanoides acutus*) and large filter-feeding copepods (*Rhincalanus gigas*), strongly migrating copepods (*Metridia* spp.). See Table 2 for a summary of experiments. Copepod mortality in experiments ranged from 0 to 26% (mean 9%).

The concentrations of different cell types in 5 mL of the preserved microplankton samples were counted using a FlowCam 8400 (Yokogawa Fluid Imaging Technologies Inc.) fitted with a 10x objective and a FOV100 flow cell, at a flow rate of 0.25 mL min^{-1}. Images were collected using auto-image mode at a rate of 37 frames per second. For the experiment using water collected at 350m, where particle concentrations were low compared to the surface, samples were settled for 48 h, and reduced to 50% of the original volume before analysis. Libraries of dominant cell types were created and used in conjunction with size filters to classify particles automatically into broad taxonomic groups (flagellates, small dinoflagellates, large athecate dinoflagellates, large thecate dinoflagellates, ciliates, pennate diatoms, centric diatoms and unidentified cells) using VisualSpreadsheet software (Version 4.3.55). Automatic classifications were checked manually, and corrected when necessary (~50% of particles). Biomass (μg C) was calculated using particle volume (μm^3) and published carbon to volume relationships (Alldredge, 1998; Menden-Deuer and Lessard, 2000). Ingestion rates were calculated using the equations of Frost (1972) and converted to carbon specific ingestion rates using published estimates of copepod's biomass (Ward et al., 2012).

2.5.2. Total community ingestion

Carbon specific ingestion rates (d^{-1}) were applied to the biomass of appropriate taxa from net samples to calculate total daily ingestion rates m^{-3}. For *Oithona*, ingestion rates measured using deep water were applied to deep nets; for all other taxa we applied ingestion rates measured using surface water throughout the water column. As we could not feasibly measure ingestion rates for all species, measured copepod specific ingestion rates (see above) were applied to the biomass of other copepods sharing similar body size and feeding traits (Table 2). Published values for specific ingestion rates (daily ration), measured in polar and sub-polar regions, were used for species or groups from Bongo, MOCNESS and RMT25 samples for which we did not measure ingestion (see Supplementary Table S6). Since the mesopelagic fish community in the Scotia Sea is dominated by myctophids and bathylagids (Collins et al., 2012) we applied a single daily ration to all fish species. A daily ration of 3% was used for categories for which there was no suitable data available in the literature (appendicularians, barnacle nauplii, carnivorous copepods such as Euchaetidae, cnidarians, gastropods, isopods, mysids, cladocerans and polychaetes) based on the mean of the other compiled data (see Supplementary Table S6, excluding *Oithona similis* and *Salpa thomsoni* which had daily rations >20%). Only ingestion for Bongo net particles less than 300 μm were included to avoid overlap with the MOCNESS ingestion estimates.

2.6. Lipid analysis

Calanoides acutus C5 and *Rhincalanus gigas* C6 female lipid extractions were carried out on each homogenised freeze-dried ($-60°C$; 10^{-2} mBar) sample (1–60 mg). An internal standard (30–100 μL of 5α(H)-cholestane; 101 ng μL^{-1}) was added to each sample, followed by a mixture of dichloromethane (DCM) and methanol (9:1; 15 mL). The samples were then sonicated (15 min, x2) and the resulting extract was

decanted into round bottom flasks. The solvent obtained was evaporated to dryness under vacuum using a rotary evaporator at ~30°C. Each sample was then passed through a Pasteur pipette filled with anhydrous sodium sulphate using DCM (3 mL). The solvent was blown down with nitrogen gas and the samples were stored (−20°C) before transmethylation and derivatisation with BSTFA.

GC-MS analyses were conducted using a GC Trace 1300 fitted with a split-splitless injector and column DB-5MS (60m x 0.25 mm (i.d.), with film thickness 0.1 μm, non-polar stationary phase of 5% phenyl and 95% methyl silicone), using helium as a carrier gas (2 mL min^{-1}). The GC oven was programmed after 1 min from 60°C to 170°C at 6°C min^{-1}, then from 170°C to 315°C at 2.5 °C min^{-1} and held at 315 °C for 15 min. The eluent from the GC was transferred directly via a transfer line (320°C) to the electron impact source of a Thermoquest ISQMS single quadrupole mass spectrometer. Typical operating conditions were: ionisation potential 70 eV; source temperature 215°C; trap current 300 μA. Mass data was collected at a resolution of 600, cycling every second from 50 to 600 Da and were processed using Xcalibur software.

Compounds were identified either by comparison of their mass spectra and relative retention indices with those available in the literature and/or by comparison with authentic standards. Quantitative data were calculated by comparison of peak areas of the internal standard with those of the compounds of interest, using the total ion current (TIC) chromatogram. The relative response factors of the analytes were determined individually for 36 representative fatty acids, sterols and an alkenone using authentic standards. Response factors for analytes where standards were unavailable were assumed to be identical to those of available compounds of the same class.

2.7. Data analysis

Given the inherent patchiness in zooplankton and micronekton distribution and abundance, we have limited the statistical analyses of these complex communities and therefore do not extend our conclusions beyond the data available. The total biomass of mesozooplankton and micronekton did not change from P3A to P3C suggesting that our measurements can be treated as replicate occupations of station P3 rather than separate stations. Wilcoxon rank sum tests were used to test whether the total lipid content of *C. acutus* and *R. gigas* changed between stations P3B and P3C. Spearman's correlation was used to test whether total pelagic community respiration and ingestion rates were correlated.

3. Results

Detailed description of the sampling environment can be found in Ainsworth et al. (2023) and Giering et al. (2023). In brief, there were deeper mixed layers during P3A and P3B (70m) compared to P3C (60m). Water column temperature was fairly consistent (surface = 2.3–3.6 °C, upper mesopelagic = 0.8–1.5 °C). Surface chlorophyll concentration decreased from station P3A to P3C, but remained high throughout the sampling period (>1 mg m^{-3}) (Ainsworth et al., 2023). The subsurface chlorophyll depth (mean = 32 ± 14m) and concentration (mean = 3.5 ± 1.8 mgm^{-3}) were variable, even within stations. POC concentrations at the surface declined from station P3A to P3C, whilst concentrations in the upper mesopelagic increased during this time (Giering et al., 2023). Mean day length was 16 h ±30 min and lunar phase was 'new' during P3A, 'full' during P3B and 'last quarter' during P3C.

3.1. Biomass

The greatest concentration of biomass, by three orders of magnitude, was found in mesozooplankton samples taken by the MOCNESS (>330 μm). The ranges of biomass found in Bongo (>100 μm), MOCNESS (>330 μm) and RMT25 (>4 mm) net samples were 0.08–0.13, 17.9–47.1 and 0.11–1.19 mmolC m^{-3} (0.96–1.62, 214.8–565.1 and 1.38–2.27 mgC m^{-3}) respectively; hereafter biomass data are given in molar units of

carbon. The biomass in Bongo net samples was dominated by large copepods and polychaetes (predominantly *Pelagobia* spp.) at both depths (Fig. 1). The surface MOCNESS samples were dominated by *Calanoides acutus* stages C4-5 (mean 74% of total biomass from the MOCNESS, Fig. 1). In the rest of the water column *C. acutus* C4-5 and *Rhincalanus gigas* C6 females constituted a mean 32–43% of total biomass from the MOCNESS. The remainder of the biomass was made up of a number of different species which individually contributed <5% to the total biomass. Mesopelagic *Bathylagus* spp., myctophids (*Krefftichthys anderssoni*, *Gymnoscopelus braueri*, *Electrona antarctica* and *Protomyctophum tenesoni*), other fish and euphausiids formed >80% of the biomass from RMT25 nets, with the fish being more dominant in the deeper samples (Fig. 1). There were no obvious changes to the broad taxonomic composition of mesozooplankton and micronekton biomass over the duration of the cruise.
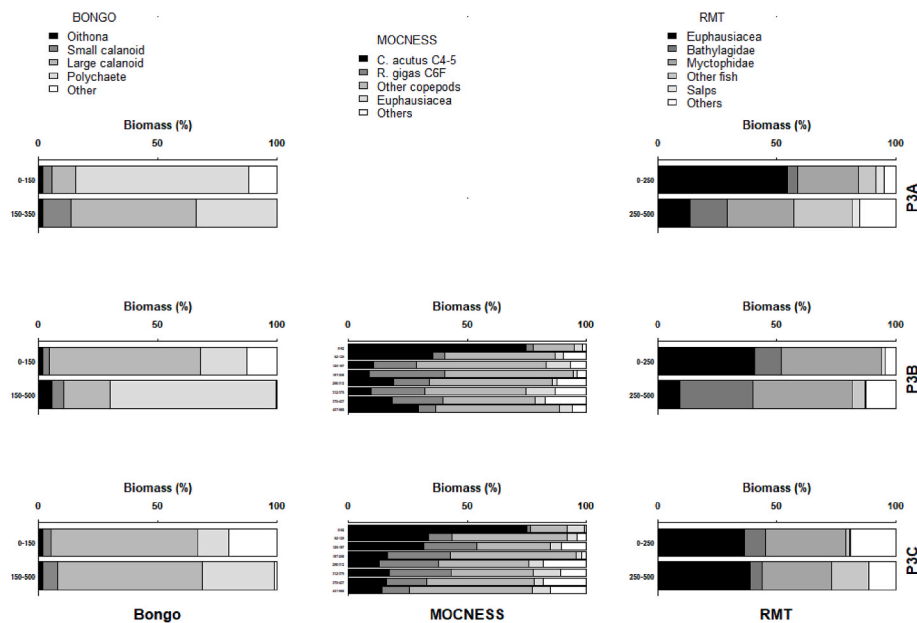
The total biomass of mesozooplankton and micronekton did not change from P3A to P3C (Fig. 2). Day/night profiles of total mesozooplankton and micronekton biomass showed no consistent evidence of synchronised DVM (Fig. 2, Supplementary Figs. 1 and 2). The biomass at night ranged between 28 and 183% of that during the day, with a mean of 95.2 ± 63.2%. In general, there was greater biomass in the surface samples compared to deeper samples during both the day and night. The change in weighted mean depth (ΔWMD) between day and night was <50 m for total biomass of mesozooplankton from the MOCNESS net and micronekton from the RMT25 net (Fig. 3), with no consistency in whether total biomass was deeper or shallower during the day. When considering specific taxa, there were consistent depth changes for appendicularians (shallower during the day by < 50m), *Metridia* spp. (deeper during the day by 20–110m), salps (deeper during the day by 50–140m), bathylagids, myctophids and other fish (deeper during the day by 50–115m) and decapods (deeper during the day by 10–110m).

Vertical profiles of acoustic backscatter at 18 and 38 kHz (indicating fish and micronekton) showed little or no evidence of synchronised DVM of the deep scattering layers (e.g. 250 m, 450 m and 700m) during P3A and P3B, although there was greater biomass at night in the top 50m compared to the day (Supplementary Figs. S1 and S2). There was evidence for day/night differences in the top 125 m of the water column in the higher frequency profiles of 120 and 200 kHz (indicating copepods and smaller euphausiids). In general, there was more backscatter in surface waters at night, but it was not possible to discern which depth it had originated.

3.2. Respiration

Mean (± s.d.) mesozooplankton daily carbon specific respiration rates at *in situ* temperatures, 0.9–3.2 °C, were 0.96 ± 0.77% d^{-1}. For comparison with wider literature we calculated respiration rates at 20 °C, using a standard Q_{10} of 2 (although see Maas et al., 2021), giving a mean (± s.d.) mesozooplankton daily specific respiration rate at 20 °C of 3.3 ± 2.5% d^{-1}. Specific respiration at the *in situ* temperature in Bongo net samples during P3C ranged between 0.15 and 0.95% d^{-1}. Specific respiration rates in Mammoth samples at the *in situ* temperature were higher during P3C (0.31–3.8% d^{-1}) than P3A (0.10–1.7% d^{-1}). Carbon specific respiration rates were highest in surface samples, decreased with depth to a minimum at around 400m, and were on average 9% higher during the day compared to the night (Supplementary Fig. S3).

Total community respiration in Bongo (>100 μm), MOCNESS (>330 μm) and RMT25 (>4 mm) net samples ranged between 0.03-0.09, 0.31–1.40 and 0.002–0.02 mmolC m^{-3} d^{-1} (0.34–1.04, 3.69–16.81 and 0.02–0.20 mgC m^{-3} d^{-1}) respectively. Pelagic respiration (mmolC m^{-3} d^{-1}) was dominated by the >330 μm mesozooplankton from the MOCNESS samples (Fig. 4) and was higher in surface samples compared to deeper samples from all net types. Total mesozooplankton respiration was higher during P3C compared to the other stations in Bongo

Fig. 1. Dominant taxa (by % of total carbon biomass) of mesozooplankton (Bongo net >100 μm; MOCNESS >330 μm) and micronekton (RMT25 >4 mm) biomass at station P3 (A–C) in the Scotia Sea (day and night combined). The 'Euphausiacea' category consisted of all species except *Euphausia superba* in the MOCNESS samples, and all species including *E. superba* in the RMT samples. The 'Other' category consisted of gastropods, ostracods, appendicularians and decapod larvae in the Bongo net samples; amphipods, appendicularians, chaetognaths, ostracods, polychaetes, pteropods, salps and siphonophores in the MOCNESS samples; and amphipods, cephalopods, chaetognaths, decapods, ostracods, polychaetes, and pteropods in the RMT samples.
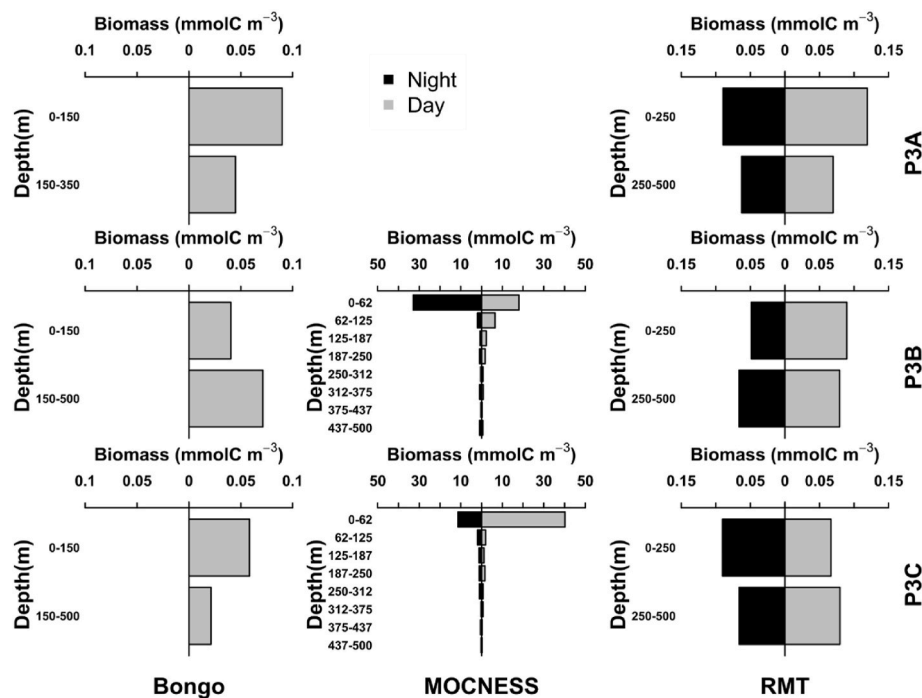
Fig. 2. Carbon biomass (mmolC m^{-3}) of mesozooplankton (Bongo net >100 μm; MOCNESS >330 μm) and micronekton (RMT25 >4 mm) at station P3 (A–C) in the Scotia Sea. Note the different scales on the x-axes. MOCNESS biomass samples were not collected during P3A.

(maximum 0.02, 0.02, 0.07 mmolC m^{-3} d^{-1} during P3A, B, C respectively) and MOCNESS (maximum 0.24, 1.33 mmolCm^{-3}d^{-1} during P3B, C respectively) mesozooplankton samples. Micronekton respiration from the RMT25 samples was dominated by euphausiid respiration but was very low compared to mesozooplankton respiration. Micronekton respiration was lowest during P3A (maximum 0.0008 mmolCm^{-3}d^{-1}; 0.01 mgC m^{-3} d^{-1}), highest during P3B (maximum 0.01 mmolCm^{-3}d^{-1}; 0.18 mgC m^{-3} d^{-1}) and was always higher at night compared to the day.

3.3. Ingestion

The phytoplankton community was dominated by diatoms larger than 10 μm (*Chaetoceros* spp., *Thalassionema nitzschioides, Fragilariopsis kerguelensis, Eucampia antarctica*, and *Pseudo-nitzschia* spp.) throughout the study period with cell counts >500 cells mL^{-1} (Ainsworth et al., 2023). This was also apparent in the experimental incubation water collected from the surface (Supplementary Fig. S4A), but deep incubation water was dominated by flagellates and unidentified particulate matter.

Carbon specific ingestion rates measured ranged between 0.13 and 145% d^{-1}. Mean carbon specific ingestion rates of *O. similis* were always high compared to the other copepod species measured (Supplementary Fig. S4B, Supplementary Table S6) and were on average three times higher in younger *O. similis* stages (C3-4: 55.4–145.9% d^{-1}) compared to
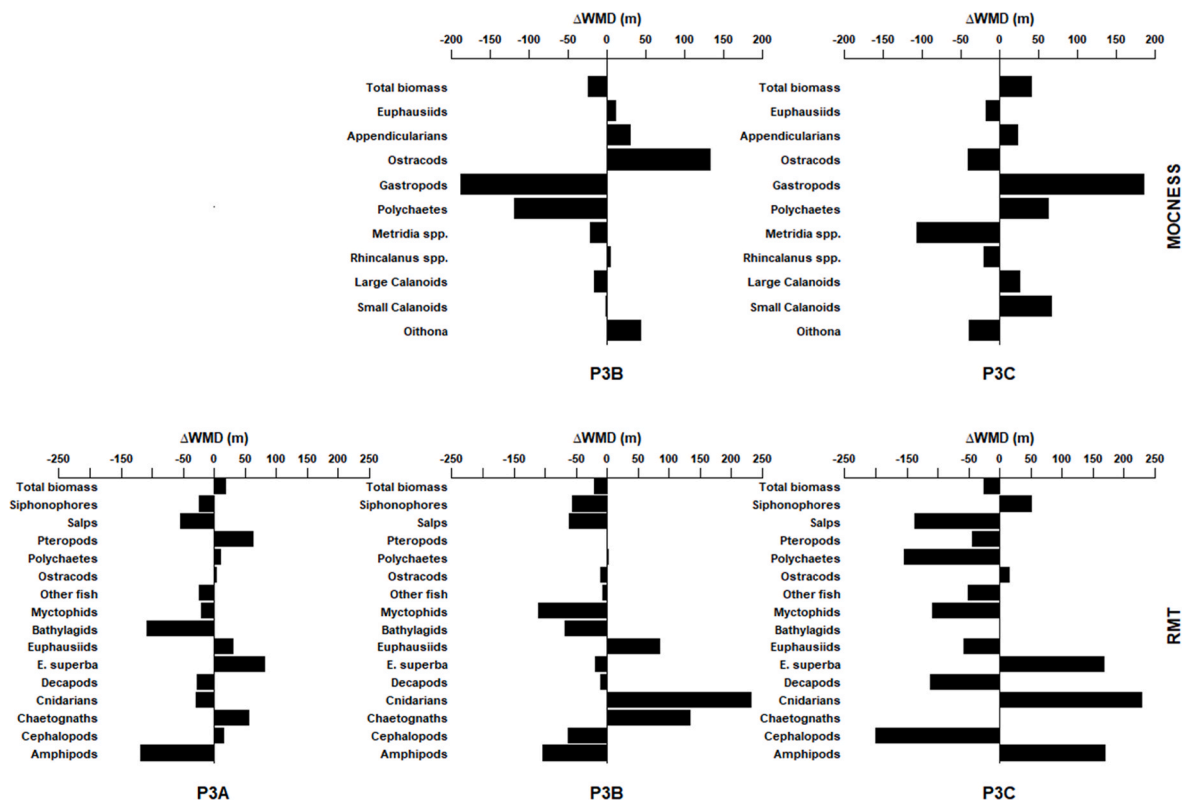
Fig. 3. Difference in day and night Weighted Mean Depth (ΔWMD, m) of dominant taxa collected by the MOCNESS (>330 μm) and RMT25 net (>4 mm) during stations P3A, P3B and P3C. Negative values indicate deeper WMD during the day. MOCNESS biomass samples were not collected during P3A.

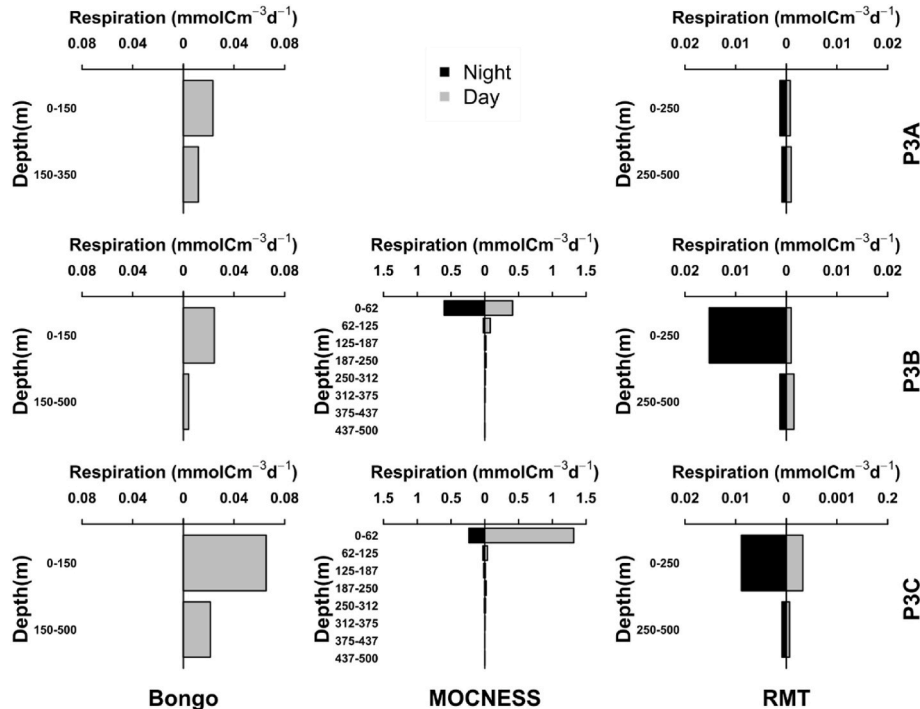**Fig. 4.** Total community respiration (mmolC m^{-3} d^{-1}) of mesozooplankton (Bongo net >100 μm; MOCNESS >330 μm) and micronekton (RMT25 >4 mm) at station P3 (A–C) in the Scotia Sea. Note the different scales on the x-axes.

older stages (C5-6: 2.4–59.0% d^{-1}). *Ctenocalanus* spp. and *Metridia* spp. had intermediate carbon specific ingestion rates (7.7–11.2 and 5.1–10.6% d^{-1} respectively), whilst *C. acutus* and *R. gigas* consistently

had low carbon specific ingestion rates (0.1–2.3 and 0.4–7.7% d^{-1} respectively).

Oithona similis (all stages measured) incubated in water collected

from the chlorophyll maximum ingested a high percentage of unidentified cells (45.4–59.1% of total carbon ingested) which was largely made up of phytodetritus, faecal pellets and aggregates (Supplementary Fig. S4A). The rest of their diet was a mix of diatoms and dinoflagellates, with some ciliates. The only exception to this was during P3A for *O. similis* incubated in water collected at the surface, where 86.9% of the diet was diatoms. *O. similis* incubated with water collected at 350m ingested unidentified cells (66.7%) and ciliates (25.0%). Diatoms were the largest component of the diet for all *C. acutus* (45.4–60.9%), *R. gigas* (37.5–70.0%) and *Ctenocalanus* spp. (48.7%) (Supplementary Fig. S4A). For both *C. acutus* and *R. gigas,* the rest of the diet was mainly composed of ciliates during P3B (31.4% and 24.7% respectively) and dinoflagellates during P3C (28.0% and 24.9% respectively). The diet of *Metridia* spp. was fairly evenly split between diatoms (35.2%), dinoflagellates (28.0%) and ciliates (32.7%) (Supplementary Fig. S4A). There were few consistent patterns in feeding selectivity, however *O. similis* tended to select against large thecate dinoflagellates, preferring ciliates and phytodetrital aggregates, whilst all other copepods selected for large thecate dinoflagellates and against phytodetrital aggregates.

Total community ingestion in Bongo (>100 μm), MOCNESS (>330 μm) and RMT25 (>4 mm) net samples ranged between 0.003 and 0.007, 0.53–1.30, 0.004–0.010 mmolC m^{-3} d^{-1} (0.03–0.09, 6.34–15.63 and 0.05–0.12 mgC m^{-3} d^{-1}) respectively. Pelagic ingestion was dominated by that of mesozooplankton >330 μm from the MOCNESS samples (Fig. 5). Total ingestion from these MOCNESS samples was always higher in surface samples compared to deep samples reflecting the higher biomass in these nets. There was no substantial change in ingestion rates over time.

3.4. Lipid content

The total lipid content (mg total lipid per g organic carbon (OC)) of *C. acutus* changed from 924.1 ± 233.9 to 785.1 ± 232.5 mg g^{-1} OC between P3B (n = 3) and P3C (n = 3), respectively, although this decrease was not significant (Wilcoxon rank sum test, W = 6, p = 0.35, Table 4). For *R. gigas* however, there was a significant decrease in total lipid content from 798.1 ± 138.0 to 500.1 ± 51.3 mg g^{-1} OC between

P3B (n = 4) and P3C (n = 3), respectively (Wilcoxon rank sum test, W = 12, p < 0.05, Table 3).
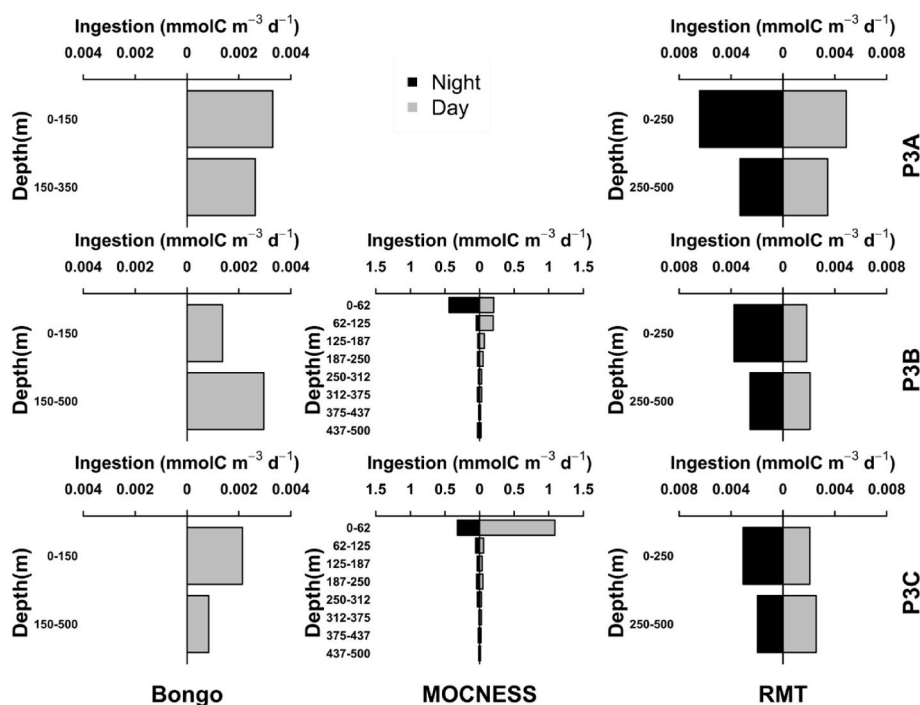
3.5. Carbon budgets of the mesopelagic zooplankton and nekton communities in the Scotia Sea

Total pelagic community respiration and ingestion rates were within the same order of magnitude (Fig. 6) and were highly positively correlated (Spearman correlation r = 0.81, p < 0.05, N = 16). These metabolic rates did not vary with station or time of day in deep samples where ingestion rates were always higher than respiration rates (mean ingestion = 0.08 ± 0.009 mmolC m^{-3} d^{-1}, mean respiration = 0.02 ± 0.001 mmolC m^{-3} d^{-1}). There was higher variability in the metabolic rates from shallow samples. Rates were lower during P3B (mean ingestion = 0.54 ± 0.02 mmolC m^{-3} d^{-1}, mean respiration = 0.58 ± 0.08 mmolC m^{-3} d^{-1}), than during P3C (mean ingestion = 0.84 ± 0.55 mmolC m^{-3} d^{-1}, mean respiration = 0.84 ± 0.77 mmolC m^{-3} d^{-1}). Though there was no consistent day/night change during P3B, the

Table 3
Total lipid content (mg total lipid per g organic carbon (OC)) of copepods *Calanoides acutus* stage C5 and *Rhincalanus gigas* stage C6 female collected from MOCNESS tows during stations P3B and P3C.

| Species	Station	MOCNESS Event	Depth	Total lipid content (mg g^{-1} OC)
Calanoides acutus C5	P3B	217	0–62m	918.6
		234	187–250m	693.0
		217	437–500m	1160.7
	P3C	315	0–62m	1045.1
		315	125–187m	597.3
		315	375–437m	712.8
Rhincalanus gigas C6F	P3B	234	0–62m	612.7
		217	187–250m	928.0
		217	250–312m	779.4
		234	375–437m	872.3
	P3C	315	125–187m	539.3
		315	250–312m	518.9
		315	375–437m	442.1

Fig. 5. Total community ingestion (mmolC m^{-3} d^{-1}) of mesozooplankton (Bongo net >100 μm; MOCNESS >330 μm) and micronekton (RMT25 >4 mm) at station P3 (A–C) in the Scotia Sea. Note the different scales on the x-axes.

Table 4

P3 metabolic budgets. Estimated total mesozooplankton and micronekton community rates of respiration (R, mmolC m^{-3} d^{-1}), calculated using respiratory quotients (RQ) of 0.9 and 0.7, and ingestion (I, mmolC m^{-3} d^{-1}).

			P3B		P3C	
			250–350	0–250	250–500	0–250
R (mmolC m^{-3} d^{-1})	RQ = 0.9	Night	0.016	0.64	0.017	0.29
		Day	0.015	0.52	0.018	1.38
	RQ = 0.7	Night	0.013	0.50	0.013	0.23
		Day	0.012	0.41	0.015	1.10
I (mmolC m^{-3} d^{-1})		Night	0.095	0.55	0.076	0.46
		Day	0.089	0.52	0.078	1.23
R:I	RQ = 0.9	Night	0.17	1.17	0.22	0.64
		Day	0.17	1.00	0.24	1.13
	RQ = 0.7	Night	0.14	0.91	0.17	0.50
		Day	0.13	0.78	0.19	0.88
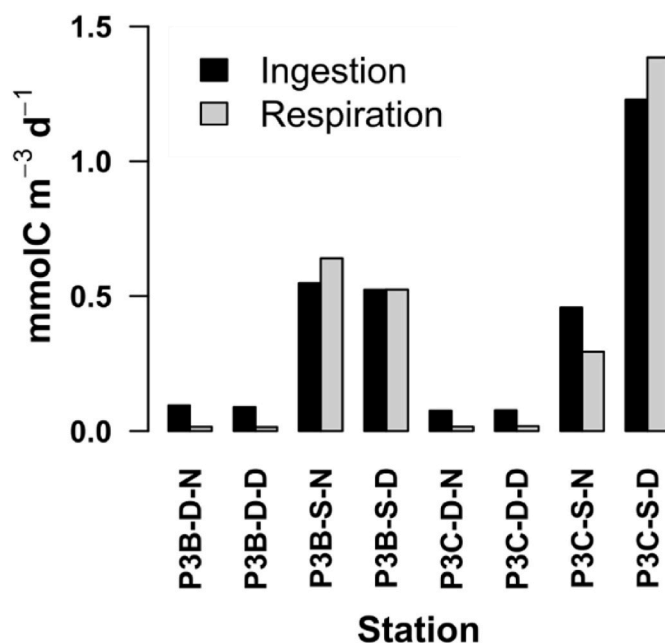
Fig. 6. Total pelagic community ingestion and respiration (mmolC m^{-3} d^{-1}) at station P3 in the Scotia Sea. P3B-D-N = station P3B deep night, P3B-D-D = station P3B deep day, P3B–S–N = station P3B shallow night, P3B–S-D = station P3B shallow day, P3C-D-N = station P3C deep night, P3C-D-D = station P3C deep day, P3C–S–N = station P3C shallow night, P3C–S-D = station P3C shallow day. Deep = 250–500m, shallow = 0–250m.

daytime metabolic rates during P3C were 3–5 times higher than those during the night. Respiration rates were only lower than ingestion rates in shallow samples on one occasion.

4. Discussion

Quantifying the vertical distribution and movements of zooplankton, along with their feeding behaviours and metabolic requirements, is integral to understanding how ocean biology contributes to the biological carbon pump (Steinberg and Landry, 2017). We quantified the magnitude of diel vertical migration (DVM) and physiological rates of mesozooplankton and micronekton communities off South Georgia in the Scotia Sea (S. Atlantic) in order to contribute to a synthesis of the mesopelagic carbon budget at this site (Giering et al., 2023). There was an apparent excess of ingested carbon relative to metabolic requirements in the deep samples, but total community respiration was greater than ingestion for most shallow samples suggesting a potential metabolic imbalance in surface waters consistent with the observation

that flux attenuation was greater than POC accumulation in the shallow mesopelagic (Giering et al., 2023).

4.1. Biomass and DVM

Total integrated biomass estimates, for stations where there was a complete suite of net measurements (Fig. 2), were towards the high end of previous estimates in the same area (Ward et al., 2012). The biomass dominance of intermediate and large calanoid copepods (*Calanoides acutus* and *Rhincalanus gigas*) in the mesozooplankton, and euphausiids, bathylagid and myctophid fish in the micronekton (Fig. 1) is also consistent with the literature (e.g. Atkinson et al., 2012; Collins et al., 2012; Ward et al., 2012).

We found little evidence of any synchronised DVM at the population level using the biomass data (Figs. 2–3). This may be consistent with the satiation sinking hypothesis (Tarling and Johnson, 2006; Tarling and Thorpe, 2017), where individuals asynchronously swim to the surface to feed and passively sink once satiated. The bulk of the mesozooplankton/micronekton biomass was consistently found in the top 62 m except for taxa that underwent synchronised DVM (*Metridia* spp., salps, bathylagids, myctophids, other fish and decapods). The acoustics data (Supplementary Figs. S1–2) also provided little evidence of synchronised DVM in the fish and large micronekton (as evidenced by the 18 and 38 kHz). It is possible that vertical migration was still taking place in an unsynchronised manner over the day night cycle, but this was not resolved by the techniques available to us during the present study.

DVM is a behavioural response to a combination of exogenous factors (e.g., light, temperature, salinity, and oxygen) and endogenous factors (e.g. sex, age, satiation, and physiology) (Forward, 1988) thought to maximise feeding opportunities whilst minimising predation risk (e.g. De Robertis, 2002; Hansen and Visser, 2016). Studies in the Antarctic have shown variable presence of DVM (e.g. Conroy et al., 2020; Kwong et al., 2020 and references therein) and it has been proposed that phytoplankton blooms can halt DVM (Cisewski et al., 2010; Cisewski and Strass, 2016) or that the apparent lack of DVM can result from not sampling the right depths (Flores et al., 2014). Omand et al. (2021) recently reported upward migrations of animals at ~300m driven by cloud shadows which could also have impacted behaviours during our study (Platnick et al., 2015). In the case of the lipid-storing copepod species, *C. acutus*, which dominated the mesozooplankton biomass, the absence of synchronised DVM may also indicate that a proportion of their population was still in the process of emerging from diapause. This is consistent with the observed phenology of *C. acutus* in the vicinity of our sampling location (Supplementary Fig. S5), where animals typically exit diapause between November and December. However, at the community scale, it seems most likely that the lack of synchronised DVM was due to the excellent feeding conditions in the surface waters and resulting high levels of high quality POM throughout the water column (Giering et al., 2023) as has previously been observed during spring blooms in the Lazarev and Weddell seas (Cisewski et al., 2010; Cisewski and Strass, 2016).

One of the challenges for identifying patterns of synchronised DVM in micronekton and particularly myctophid fish is active net avoidance (Kaartvedt et al., 2012) and the depth at which they reside during the day (>500m; Cotté et al., 2022). Many studies use only night time nets to determine fish biomass (e.g. Collins et al., 2012), noting that daytime avoidance of pelagic nets is common and biases our understanding of DVM. It should also be noted that our nets were limited to the top 500 m of the water column, and DVM can occur at depths greater than this. However, whilst scattering layers were observed below 500 m at 700m water depth, there was also no evidence of day/night differences in the intensity or depth of these layers indicating limited migration to shallower waters.

4.2. Physiological rates

Temperature-corrected (to 20 °C using $Q_{10} = 2$, see section 3.3) daily carbon specific respiration rates for mesozooplankton were consistent with published values and showed a decrease with depth, as reported previously (Steinberg et al., 2000; Ikeda et al., 2006; Yebra et al., 2018; Hernández-León et al., 2019a, 2019c; Landry et al., 2020). Exactly what drives this apparently common trend is unclear. The temperature-dependence of their respiration rates (Ikeda, 1985, 2014) provides a potential explanation, although the lack of a clear relationship between water temperature and specific respiration (Supplementary Fig. S3) suggests that this is not the only driver. Belcher et al. (2020) similarly found that temperature was a less significant driver of respiration rates over the small temperature range found in the Scotia Sea compared to areas with larger temperature gradients. Specific respiration rates also scale as a function of biomass, with larger animals having lower rates than their smaller counterparts (e.g. Kiørboe and Hirst, 2014). The biomass in our surface nets was dominated by the intermediate-sized ($\sim$30 μmol C copepod^{-1}) *C. acutus*, whereas the deeper nets showed increasing contributions of the far larger ($\sim$88.3 μmol C copepod^{-1}) *R. gigas*. This shift towards an increasing contribution of large copepods at greater depths is generally consistent with the idea that the observed decrease in specific respiration rates may be attributable to a shift in the size structure of the zooplankton community. An additional, non-mutually exclusive explanation for the decline in specific respiration with depth is that an increasing fraction of both *R. gigas* and *C. acutus* in the deeper nets were still in, or in the process of emerging from, diapause, during which respiration rates are significantly lower (Hirche, 1984; Drits et al., 1994; Supplementary Fig. S5). Unfortunately, our ETS-based estimates of respiration in the MOCNESS nets, where these species dominated, were generated using bulk community samples, and therefore it is not possible to explore this idea further.

Total respiration rates in the deep samples (0.015–0.018 mmolC m^{-3} d^{-1}; 0.18–0.22 mgC m^{-3} d^{-1}, Fig. 4) were also comparable to previous studies using direct measurements, e.g. 0.014–0.067 mmolC m^{-3} d^{-1} (0.17–0.80 mgC m^{-3} d^{-1}) in the SW Mediterranean (Yebra et al., 2018) and 0.024–0.051 mmolC m^{-3} d^{-1} (0.29–0.62 mgC m^{-3} d^{-1}) in the Southern Ocean (Mayzaud et al., 2002b). By contrast, total respiration rates in surface samples (0.29–1.38 mmolC m^{-3} d^{-1}; 3.52–16.6 mgC m^{-3} d^{-1}, Fig. 4) were at least an order of magnitude higher than previous studies, although we recognise that published rates vary considerably depending on the methods employed (Hernández-León and Gómez, 1996; Hernández-León and Ikeda, 2005; Bondyale-Juez et al., 2017; Belcher et al., 2020). We estimated respiration using a combination of allometric equations and ETS assays, both of which will have introduced a number of uncertainties beyond those associated with methods employed to generate the underlying estimates of biomass. For example, R:ETS ratios in the literature range from 0.16 to 2.55 (Hernández-León and Gómez, 1996; Osma et al., 2016a, 2016b; Bondyale-Juez et al., 2017), although ratios measured in the laboratory with cultured animals are rarely >1. We used a fixed R:ETS ratio of 0.5, which is considered conservative (Ikeda, 1985; Hernández-León and Gómez, 1996), and assumed constant respiration during day and night. However, Belcher et al. (2020) calculated an R:ETS ratio of 0.14 for the mesopelagic fish the Scotia Sea (based on ETS measurements and allometrically derived respiration rates) so it may be that 0.5 is excessive. An R:ETS ration of 0.14 would result in a 72% decrease in estimated respiration if applied to all taxa, or a 2–40% decrease in estimated micronekton (RMT25) respiration if applied only to fish. In addition, Belcher et al. (2019b) found notable variability in the respiration rates of mesopelagic fish in the Scotia Sea which was not apparent in allometrically-based estimates, suggesting that allometric estimates may not capture the true scale of variability which could introduce errors that propagate when generating population-scale estimates. We converted estimated values of oxygen consumption into carbon units using a fixed RQ of 0.9, based on the assumption that the sampled animals were respiring proteins and carbohydrates (Prosser, 1961). However, the prevalence of *C. acutus* stage 5 copepodites with substantial lipid reserves throughout the water column (Fig. 1, Table 3) suggests that a proportion of the community was emerging from diapause and thus still using lipid-based metabolism. In this case, an RQ of $\sim$0.7 may have been more appropriate (Prosser, 1961), and therefore our assumed value of RQ = 0.9 would have overestimated respiration rates considerably (see Section 4.3, below).

Daily specific ingestion rates of the copepod species examined generally agreed well with previous studies, although rates for *C. acutus* were towards the lower end of published values (Atkinson et al., 1992, 1996; Swadling et al., 1997; Hernández-León et al., 2000; Bernard and Froneman, 2003; Sarthou et al., 2008). The highest specific ingestion rates were found in the smaller species, e.g. *Oithona similis* and lowest in the largest (*Rhincalanus gigas*), consistent with metabolic scaling theory (Kiørboe and Hirst, 2014). The low ingestion rates for *C. acutus* stage C5 may again be because many of these individuals were still in the process of breaking the winter dormancy, although low ingestion rates for this species are not uncommon (e.g. Drits et al., 1994; Mayzaud et al., 2002a). Patterns in feeding selectivity were also consistent with those in the literature, with *Oithona* spp. and *Metridia* spp. showing preference for motile prey, and *C. acutus* and *R. gigas* feeding mainly on diatoms (Atkinson, 1995; Atkinson et al., 2012). Our results also suggest that *Oithona* spp. fed substantially on phytodetritus, faecal pellets and aggregates (the 'unidentified particles' category) which represented $\sim$50% of their total diet. These types of particles cannot easily be counted using microscopy with settled samples, the traditional way of enumerating cells in particle removal grazing experiments. The FlowCam, however, can count these particles and provides an image for each, which can be used as a means to estimate volume and subsequently carbon content. Including these particles in grazing estimates does, however, introduce caveats. In the absence of alternative information, we used a single volume to carbon relationship for phytodetrital aggregates to estimate the carbon content in all unidentified particles. It is possible that this could both over-estimate (e.g. aggregates dominated by empty diatom frustules) and under-estimate (e.g. aggregates containing live dinoflagellates) the carbon content of such particles. Particle fragmentation by these and other particle-associated copepods has been proposed as an important mechanism for supporting their nutritional requirements (Mayor et al., 2014) and attenuating sinking flux in the mesopelagic (Mayor et al., 2020). Therefore these 'unidentified particles' could result from copepod feeding behaviour during the incubations causing particle disaggregation. By contrast, rotation of bottles on the plankton wheel could have led to the aggregation of smaller particles into larger ones over the duration of the incubations, with any such effects differing between the control and experimental bottles if the incubated copepods were fragmenting particles. More detailed observations of how small, particle-associated copepods interact with particles, alongside a better understanding of how particle composition relates to its elemental and biochemical composition, are clear priorities for future mesopelagic research (Koski et al., 2017, 2020; Mayor et al., 2020).

As for total respiration, total ingestion rates in deep samples (250–500m; Fig. 5; Table 4) were comparable to previous studies (Swadling et al., 1997; Mayzaud et al., 2002b; Pakhomov et al., 2002). Total community ingestion rates in surface samples (0–250m; Fig. 5; Table 4) were at least an order of magnitude higher than those in deep samples and were more comparable to maximum rates found in Antarctic coastal waters (Swadling et al., 1997). When calculating ingestion rates, we assumed that animals were feeding at depth since we found no clear evidence of synchronised DVM and significant flagellate concentrations were observed at 350m (Supplementary Fig. S4A). We applied the same biomass-specific ingestion rate to surface and deep biomass measurements which may have resulted in an overestimation of the total community ingestion over the water column since most ingestion

experiments used water collected from near surface. We did quantify ingestion rates for *Oithona* spp. incubated with water collected at depth (350m) and found slightly lower mean specific ingestion rates compared to surface waters (Supplementary Fig. S4B).

4.3. Metabolic budgets

Total mesozooplankton and micronekton community respiration and ingestion estimates were always within the same order of magnitude. Respiration accounted for between 17.0 and 23.5% of the total ingested carbon in the deep samples (Table 4), suggesting that the food ingested was more than sufficient to meet the observed metabolic requirements. The apparent excess of ingested carbon relative to respiratory requirements at depth supports the observation that food (POM) quality is poor in the mesopelagic relative to the mixed layer (based on the relative concentrations of polyunsaturated fatty acids; C. Preece and G. Wolff, personal communication), and organisms therefore have to consume a larger quantity of food in order to fulfil their metabolic and nutritional requirements (Giering et al., 2014; Mayor et al., 2014, 2020; Anderson et al., 2017).

Ingested C needs to be sufficient to simultaneously fuel respiration, growth/reproduction and excretion/egestion so, at steady state, should be substantially higher than the respired C alone. During the night visit to P3C, the estimated total respiratory demand of the surface community was again below the total amount of carbon ingested (respiration = 64.2% of ingested carbon; Table 4), leaving an apparent metabolic deficit. Carbon absorption efficiencies in copepods are reported to range between ~35 and 90% (Mayor et al., 2011 and Supplementary Table S3 therein), indicating that although the night surface population during P3C had consumed sufficient food to meet their respiratory demands, there was little excess to support an actively growing population. By contrast, respiration was greater than or equal to ingestion for all other shallow samples (respiration = 100–117% of ingestion; Table 4). This surprising result is, in fact, consistent with several other studies, where respiration is reported to be up to ~400% of ingestion (e.g. Atkinson, 1996; Razouls et al., 1998; Mayzaud et al., 2002b). Such discrepancies have previously been attributed to the absence of sufficient prey and the consumption of non-phytoplankton material. However, neither of these explanations appear appropriate in our study, owing to the high concentrations of particles throughout the water column (Giering et al., 2023) and our attempts to quantify the removal of all cell types, including both microzooplankton and detrital particles. These results may therefore suggest that our estimated rates of respiration were excessive, or that an alternative carbon source was available.

The lipid-rich copepods, *C. acutus* and *R. gigas*, constituted between ~40 and 80% of the total mesozooplankton biomass in the shallow nets (Fig. 1), and considering that our sampling coincided with the period during which these animals exit diapause (Supplementary Fig. S5), it seems likely that the apparent discrepancy between estimated total community rates of respiration and ingestion can be at least partially attributed to these animals being somewhat reliant upon the consumption of internal lipid stores. The total lipid content of *C. acutus* and *R. gigas* decreased between P3B and P3C, although this decrease was only significant for *R. gigas*. This would simultaneously explain the low ingestion rates of these animals and produce an overestimate of respiration using our assumed RQ = 0.9. Indeed, recalculating total community respiration with an RQ of 0.7, ingestion was greater than respiration in all samples, although, in some cases, a high absorption efficiency (>90%) must be implied for there to be enough carbon to meet respiratory demands (Table 4). It should be noted, however, that our observations relate specifically to the community at P3 in spring, and may not be representative of annual carbon budgets or of those elsewhere in the Southern Ocean.

4.4. Conclusions

Synchronised Diel Vertical Migration (DVM) should not be assumed, even for taxa previously shown to undertake the behaviour. This study did not observe synchronised DVM in either total biomass or in the majority of taxa examined. This lack of synchronised DVM patterns may be due to the fact that sampling took place during mid-spring when feeding conditions in the upper 200m were good. Nevertheless, our findings do not exclude the possibility that asynchronous vertical migration was taking place during this time.

The apparent excess of ingested carbon relative to respiratory requirements in the deep mesopelagic samples supports the understanding that food quality below 200m is poor and organisms have to consume a larger quantity of food in order to fulfil their metabolic and nutritional requirements. Our results also suggest that *Oithona* spp. fed on phytodetritus, faecal pellets and aggregates. These results are consistent with particle fragmentation by copepods and microbial gardening hypotheses, which could therefore play an important role in attenuating carbon flux.

There is a need to better understand the physiology of shallow water animals when assessing carbon budgets, particularly where lipid-storing species predominate. For shallow samples, we found that ingestion rates could support respiratory demands if, when calculating total community respiration, we used an RQ of 0.7, appropriate for animals respiring lipid, rather than an RQ of 0.9, appropriate for animals respiring proteins and carbohydrates. In addition, the lipid-rich copepods, thought to be exiting diapause, had low specific ingestion rates which can be at least partially attributed to these animals being somewhat reliant upon the consumption of stored lipids.

The prevalence of lipid storing copepods substantially complicates mesopelagic carbon budgeting. Stored lipids represent carbon ingested during the previous growing season, meaning lipids are integrating over very different time scales to those that are observed in the observational field programme (e.g. vertical patterns of flux attenuation).

CRediT author statement

KC conceptualised the manuscript with support from all authors. AB, DM, GS, KC, GS, GT and SF conducted on board sample collection and processing. AB, DBJ, KC, ME and SB conducted laboratory analysis of samples. GW and RS provided supporting data and technical expertise. All authors contributed to the writing of the manuscript.

Declaration of competing interest

The authors declare that they have no known competing financial interests or personal relationships that could have appeared to influence the work reported in this paper.

Data availability

Macrozooplankton and nekton vertical distribution and abundance at the sustained observation location P3 in the northern Scotia Sea (Southern Ocean) during November and December 2017 https://doi.org/10.5285/e184e81a-e43c-424e-abec-122036ee2cfd. Micronekton and zooplankton respiration rates on COMICS Cruises DY086 and DY090 https://doi.org/10.5285/b9f5c5ec-100a-7ff0-e053-6c86abc0f494. All other data is available on request,

Appendix A. Supplementary data

Supplementary data to this article can be found online at https://doi.org/10.1016/j.dsr2.2023.105296.

References

Ainsworth, J., Poulton, A.J., Lohan, M.C., Stinchcombe, M.C., Lough, A.J.M., Moore, C. M., 2023. Iron cycling during the decline of a South Georgia diatom bloom. Deep Sea Res. Part II Top. Stud. Oceanogr. 208, 105269 https://doi.org/10.1016/j.dsr2.2023.105269.

Alldredge, A., 1998. The carbon, nitrogen and mass content of marine snow as a function of aggregate size. Deep Sea Res. Oceanogr. Res. Pap. 45, 529–541. https://doi.org/10.1016/S0967-0637(97)00048-4.

Anderson, T.R., Pond, D.W., Mayor, D.J., 2017. The role of microbes in the nutrition of detritivorous invertebrates: a stoichiometric analysis. Front. Microbiol. 7 https://doi.org/10.3389/fmicb.2016.02113.

Archibald, K.M., Siegel, D.A., Doney, S.C., 2019. Modeling the impact of zooplankton diel vertical migration on the carbon export flux of the biological pump. Global Biogeochem. Cycles 33, 181–199. https://doi.org/10.1029/2018GB005983.

Ariza, A., Garijo, J.C., Landeira, J.M., Bordes, F., Hernández-León, S., 2015. Migrant biomass and respiratory carbon flux by zooplankton and micronekton in the subtropical northeast Atlantic Ocean (Canary Islands). Prog. Oceanogr. 134, 330–342. https://doi.org/10.1016/j.pocean.2015.03.003.

Atkinson, A., 1995. Omnivory and feeding selectivity in five copepod species during spring in the Bellingshausen Sea, Antarctica. ICES (Int. Counc. Explor. Sea) J. Mar. Sci. 52, 385–396. https://doi.org/10.1016/1054-3139(95)80054-9.

Atkinson, A., 1996. Subantarctic copepods in an oceanic, low chlorophyll environment: ciliate predation, food selectivity and impact on prey populations. Mar. Ecol. Prog. Ser. 130, 85–96. https://doi.org/10.3354/meps130085.

Atkinson, A., Shreeve, R.S., Pakhomov, E.A., Priddle, J., Blight, S.P., Ward, P., 1996. Zooplankton response to a phytoplankton bloom near South Georgia, Antarctica. Mar. Ecol. Prog. Ser. 144, 195–210. https://doi.org/10.3354/meps144195.

Atkinson, A., Ward, P., Hunt, B.P.V., Pakhomov, E.A., Hosie, G.W., 2012. An overview of Southern Ocean zooplankton data: abundance, biomass, feeding and functional relationships. CCAMLR Sci. 19, 171–218.

Atkinson, A., Ward, P., Williams, R., Poulet, S.A., 1992. Feeding rates and diel vertical migration of copepods near South Georgia: comparison of shelf and oceanic sites. Mar. Biol. 114, 49–56. https://doi.org/10.1007/BF00350855.

Baker, A.d.C., Clarke, M.R., Harris, M.J., 1973. The N.I.O. combination net (RMT 1 + 8) and further developments of rectangular midwater trawls. J. Mar. Biol. Assoc. U. K. 53, 167–184. https://doi.org/10.1017/S0025315400056708.

Bandara, K., Varpe, Ø., Wijewardene, L., Tverberg, V., Eiane, K., 2021. Two hundred years of zooplankton vertical migration research. Biol. Rev. 96, 1547–1589. https://doi.org/10.1111/brv.12715.

Belcher, A., Cook, K., Bondyale-Juez, D., Stowasser, G., Fielding, S., Saunders, R.A., Mayor, D.J., et al., 2020. Respiration of mesopelagic fish: a comparison of respiratory electron transport system (ETS) measurements and allometrically calculated rates in the Southern Ocean and Benguela Current. ICES (Int. Counc. Explor. Sea) J. Mar. Sci. 77, 1672–1684. https://doi.org/10.1093/icesjms/fsaa031.

Belcher, A., Henson, S.A., Manno, C., Hill, S.L., Atkinson, A., Thorpe, S.E., Fretwell, P., et al., 2019a. Krill faecal pellets drive hidden pulses of particulate organic carbon in the marginal ice zone. Nat. Commun. 10, 889. https://doi.org/10.1038/s41467-019-08847-1.

Belcher, A., Iversen, M., Manno, C., Henson, S.A., Tarling, G.A., Sanders, R., 2016. The role of particle associated microbes in remineralization of fecal pellets in the upper mesopelagic of the Scotia Sea, Antarctica. Limnol. Oceanogr. 61, 1049–1064. https://doi.org/10.1002/lno.10269.

Belcher, A., Saunders, R.A., Tarling, G.A., 2019b. Respiration rates and active carbon flux of mesopelagic fishes (family myctophidae) in the Scotia Sea, Southern Ocean. Mar. Ecol. Prog. Ser. 610, 149–162. https://doi.org/10.3354/meps12861.

Bernard, K.S., Froneman, P.W., 2003. Mesozooplankton community structure and grazing impact in the Polar Frontal Zone of the south Indian Ocean during austral autumn 2002. Polar Biol. 26, 268–275. https://doi.org/10.1007/s00300-002-0472-x.

Bondyale-Juez, D.R., Packard, T.T., Viera-Rodríguez, M.A., Gómez, M., 2017. Respiration: comparison of the Winkler technique, O$_2$ electrodes, O$_2$ optodes and the respiratory electron transport system assay. Mar. Biol. 164, 226. https://doi.org/10.1007/s00227-017-3271-1.

Boyd, P.W., Claustre, H., Levy, M., Siegel, D.A., Weber, T., 2019. Multi-faceted particle pumps drive carbon sequestration in the ocean. Nature 568, 327–335. https://doi.org/10.1038/s41586-019-1098-2.

Briggs, N., Dall'Olmo, G., Claustre, H., 2020. Major role of particle fragmentation in regulating biological sequestration of CO$_2$ by the oceans. Science 367, 791–793. https://doi.org/10.1126/science.aay1790.

Buesseler, K.O., Lamborg, C.H., Boyd, P.W., Lam, P.J., Trull, T.W., Bidigare, R.R., Bishop, J.K.B., et al., 2007. Revisiting carbon flux through the ocean's twilight zone. Science 316, 567–570. https://doi.org/10.1126/science.1137959.

Burd, A.B., Hansell, D.A., Steinberg, D.K., Anderson, T.R., Arístegui, J., Baltar, F., Beaupré, S.R., et al., 2010. Assessing the apparent imbalance between geochemical and biochemical indicators of meso- and bathypelagic biological activity: what the @$#! is wrong with present calculations of carbon budgets? Deep-Sea Res. Part II Top. Stud. Oceanogr. 57, 1557–1571. https://doi.org/10.1016/j.dsr2.2010.02.022.

Cisewski, B., Strass, V.H., 2016. Acoustic insights into the zooplankton dynamics of the eastern Weddell Sea. Prog. Oceanogr. 144, 62–92. https://doi.org/10.1016/j.pocean.2016.03.005.

Cisewski, B., Strass, V.H., Rhein, M., Krägefsky, S., 2010. Seasonal variation of diel vertical migration of zooplankton from ADCP backscatter time series data in the Lazarev Sea, Antarctica. Deep Sea Res. Oceanogr. Res. Pap. 57, 78–94. https://doi.org/10.1016/j.dsr.2009.10.005.

Collins, M.A., Stowasser, G., Fielding, S., Shreeve, R., Xavier, J.C., Venables, H.J., Enderlein, P., et al., 2012. Latitudinal and bathymetric patterns in the distribution and abundance of mesopelagic fish in the Scotia Sea. Deep Sea Res. Part II Top. Stud. Oceanogr. 59–60, 189–198. https://doi.org/10.1016/j.dsr2.2011.07.003.

Conroy, J.A., Steinberg, D.K., Thibodeau, P.S., Schofield, O., 2020. Zooplankton diel vertical migration during Antarctic summer. Deep Sea Res. Oceanogr. Res. Pap. 162, 103324 https://doi.org/10.1016/j.dsr.2020.103324.

Cotté, C., Ariza, A., Berne, A., Habasque, J., Lebourges-Dhaussy, A., Roudaut, G., Espinasse, B., et al., 2022. Macrozooplankton and micronekton diversity and associated carbon vertical patterns and fluxes under distinct productive conditions around the Kerguelen Islands. J. Mar. Syst. 226, 103650 https://doi.org/10.1016/j.jmarsys.2021.103650.

De Robertis, A., 2002. Size-dependent visual predation risk and the timing of vertical migration: an optimization model. Limnol. Oceanogr. 47, 925–933. https://doi.org/10.4319/lo.2002.47.4.0925.

Demer, D.A., Berger, L., Bernasconi, M., Bethke, E., Boswell, K., Chu, D., Domokos, R., et al., 2015. Calibration of Acoustic Instruments, vol. 326, p. 133pp.

Drits, A.V., Pasternak, A.F., Kosobokova, K.N., 1994. Physiological characteristics of the antarctic copepod *Calanoides acutus* during late summer in the Weddell Sea. Hydrobiologia 292, 201–207. https://doi.org/10.1007/BF00229942.

Flores, H., Hunt, B.P.V., Kruse, S., Pakhomov, E.A., Siegel, V., van Franeker, J.A., Strass, V., et al., 2014. Seasonal changes in the vertical distribution and community structure of Antarctic macrozooplankton and micronekton. Deep Sea Res. Oceanogr. Res. Pap. 84, 127–141. https://doi.org/10.1016/j.dsr.2013.11.001.

Forward Jr., R.B., 1988. Diel vertical migration: zooplankton photobiology and behaviour. Oceanogr. Mar. Biol. Annu. Rev. 26, 361–393.

Francois, R.E., Garrison, G.R., 1982. Sound absorption based on ocean measurements. Part II: boric acid contribution and equation for total absorption. J. Acoust. Soc. Am. 72, 1879–1890. https://doi.org/10.1121/1.388673.

Frost, B.W., 1972. Effects of size and concentration of food particles on the feeding behaviour of the marine planktonic copepods *Calanus pacificus*. Limnol. Oceanogr. 17, 805–815. https://doi.org/10.4319/lo.1972.17.6.0805.

Giering, S., Ainsworth, J., Ashurst, D., Belcher, A., Bridger, M., Carvalho, F., Cook, K., et al., 2019a. RRS Discovery Cruise DY086, 12 November – 19 December 2017. Controls over Ocean Mesopelagic Carbon Storage. COMICS). No. 55. 265pp.

Giering, S.L.C., Sanders, R., Blackbird, S., Briggs, N., Carvalho, F., East, H., Espinola, B., et al., 2023. Vertical imbalance in organic carbon budgets is indicative of a missing vertical transfer during a phytoplankton bloom near South Georgia (COMICS). Deep Sea Res. Part II Top. Stud. Oceanogr. 209, 105277 https://doi.org/10.1016/j.dsr2.2023.105277.

Giering, S.L.C., Sanders, R., Lampitt, R.S., Anderson, T.R., Tamburini, C., Boutrif, M., Zubkov, M.V., et al., 2014. Reconciliation of the carbon budget in the ocean's twilight zone. Nature 507, 480–483. https://doi.org/10.1038/nature13123.

Giering, S.L.C., Wells, S.R., Mayers, K.M.J., Schuster, H., Cornwell, L., Fileman, E., Atkinson, A., et al., 2019b. Seasonal variation of zooplankton community structure and trophic position in the Celtic Sea: a stable isotope and biovolume spectrum approach. Prog. Oceanogr. 177, 101943 https://doi.org/10.1016/j.pocean.2018.03.012.

Gómez, M., Torres, S., Hernández-León, S., 1996. Modification of the electron transport system (ETS) method for routine measurements of respiratory rates of zooplankton. S. Afr. J. Mar. Sci. 17, 15–20. https://doi.org/10.2989/025776196784158446.

Hansen, A.N., Visser, A.W., 2016. Carbon export by vertically migrating zooplankton: an optimal behavior model. Limnol. Oceanogr. 61, 701–710. https://doi.org/10.1002/lno.10249.

Hernández-León, S., Almeida, C., Portillo-Hahnefeld, A., Gómez, M., Montero, I., 2000. Biomass and potential feeding, respiration and growth of zooplankton in the Bransfield Strait (Antarctic Peninsula) during austral summer. Polar Biol. 23, 679–690. https://doi.org/10.1007/s003000000139.

Hernández-León, S., Calles, S., Fernández de Puelles, M.L., 2019a. The estimation of metabolism in the mesopelagic zone: disentangling deep-sea zooplankton respiration. Prog. Oceanogr. 178, 102163 https://doi.org/10.1016/j.pocean.2019.102163.

Hernández-León, S., Gómez, M., 1996. Factors affecting the respiration/ETS ratio in marine zooplankton. J. Plankton Res. 18, 239–255. https://doi.org/10.1093/plankt/18.2.239.

Hernández-León, S., Ikeda, T., 2005. Zooplankton respiration. In: Giorgio, P.A.d., Williams, P.J.l. (Eds.), Respiration in Aquatic Ecosystems. Oxford University Press.

Hernández-León, S., Olivar, M.P., Fernández de Puelles, M.L., Bode, A., Castellón, A., López-Pérez, C., Tuset, V.M., et al., 2019b. Zooplankton and micronekton active flux across the tropical and subtropical Atlantic Ocean. Front. Mar. Sci. 6 https://doi.org/10.3389/fmars.2019.00535.

Hernández-León, S., Putzeys, S., Almeida, C., Bécognée, P., Marrero-Díaz, A., Arístegui, J., Yebra, L., 2019c. Carbon export through zooplankton active flux in the Canary Current. J. Mar. Syst. 189, 12–21. https://doi.org/10.1016/j.jmarsys.2018.09.002.

Hidaka, K., Kawaguchi, K., Murakami, M., Takahashi, M., 2001. Downward transport of organic carbon by diel migratory micronekton in the western equatorial Pacific:: its quantitative and qualitative importance. Deep Sea Res. Oceanogr. Res. Pap. 48, 1923–1939. https://doi.org/10.1016/S0967-0637(01)00003-6.

Hirche, H.-J., 1984. Temperature and metabolism of plankton—I. Respiration of antarctic zooplankton at different temperatures with a comparison of antarctic and nordic krill. Comp. Biochem. Physiol. Physiol. 77, 361–368. https://doi.org/10.1016/0300-9629(84)90074-4.

Ikeda, T., 1985. Metabolic rates of epipelagic marine zooplankton as a function of body mass and temperature. Mar. Biol. 85, 1–11. https://doi.org/10.1007/bf00396409.

Ikeda, T., 2014. Respiration and ammonia excretion by marine metazooplankton taxa: synthesis toward a global-bathymetric model. Mar. Biol. 161, 2753–2766. https://doi.org/10.1007/s00227-014-2540-5.

Ikeda, T., 2016. Routine metabolic rates of pelagic marine fishes and cephalopods as a function of body mass, habitat temperature and habitat depth. J. Exp. Mar. Biol. Ecol. 480, 74–86. https://doi.org/10.1016/j.jembe.2016.03.012.

Ikeda, T., Sano, F., Yamaguchi, A., Matsuishi, T., 2006. Metabolism of mesopelagic and bathypelagic copepods in the western North Pacific Ocean. Mar. Ecol. Prog. Ser. 322, 199–211. https://doi.org/10.3354/meps322199.

Kaartvedt, S., Staby, A., Aksnes, D.L., 2012. Efficient trawl avoidance by mesopelagic fishes causes large underestimation of their biomass. Mar. Ecol. Prog. Ser. 456, 1–6. https://doi.org/10.3354/meps09785.

Kelly, T.B., Davison, P.C., Goericke, R., Landry, M.R., Ohman, M.D., Stukel, M.R., 2019. The importance of mesozooplankton diel vertical migration for sustaining a mesopelagic food web. Front. Mar. Sci. 6 https://doi.org/10.3389/fmars.2019.00508.

Kiørboe, T., 2013. Zooplankton body composition. Limnol. Oceanogr. 58, 1843–1850. https://doi.org/10.4319/lo.2013.58.5.1843.

Kiørboe, T., Hirst, A.G., 2014. Shifts in mass scaling of respiration, feeding, and growth rates across life-form transitions in marine pelagic organisms. Am. Nat. 183, E118–E130. https://doi.org/10.1086/675241.

Kittel, W., Witek, Z., Czykieta, H., 1985. Distribution of *Euphausia frigida, Euphausia crystallorophias, Euphausia triacantha* and *Thysanoessa macrura* in the southern part of drake passage and in the bransfield strait during the 1983—1984 austral summer (BIOMASS-SIBEX). Pol. Polar Res. 6, 133–149.

Korb, R.E., Whitehouse, M.J., Ward, P., Gordon, M., Venables, H.J., Poulton, A.J., 2012. Regional and seasonal differences in microplankton biomass, productivity, and structure across the Scotia Sea: implications for the export of biogenic carbon. Deep Sea Res. Part II Top. Stud. Oceanogr. 59–60, 67–77. https://doi.org/10.1016/j.dsr2.2011.06.006.

Koski, M., Boutorh, J., de la Rocha, C., 2017. Feeding on dispersed vs. aggregated particles: the effect of zooplankton feeding behavior on vertical flux. PLoS One 12, e0177958. https://doi.org/10.1371/journal.pone.0177958.

Koski, M., Valencia, B., Newstead, R., Thiele, C., 2020. The missing piece of the upper mesopelagic carbon budget? Biomass, vertical distribution and feeding of aggregate-associated copepods at the PAP site. Prog. Oceanogr. 181, 102243 https://doi.org/10.1016/j.pocean.2019.102243.

Kwon, E.Y., Primeau, F., Sarmiento, J.L., 2009. The impact of remineralization depth on the air–sea carbon balance. Nat. Geosci. 2, 630–635. https://doi.org/10.1038/ngeo612.

Kwong, L.E., Henschke, N., Pakhomov, E.A., Everett, J.D., Suthers, I.M., 2020. Mesozooplankton and micronekton active carbon transport in contrasting eddies. Front. Mar. Sci. 6 https://doi.org/10.3389/fmars.2019.00825.

Landry, M.R., Stukel, M.R., Décima, M., 2020. Food-web fluxes support high rates of mesozooplankton respiration and production in the equatorial Pacific. Mar. Ecol. Prog. Ser. 652, 15–32. https://doi.org/10.3354/meps13479.

Le Moigne, F.A.C., 2019. Pathways of organic carbon downward transport by the oceanic biological carbon pump. Front. Mar. Sci. 6 https://doi.org/10.3389/fmars.2019.00634.

Liszka, C.M., Manno, C., Stowasser, G., Robinson, C., Tarling, G.A., 2019. Mesozooplankton community composition controls fecal pellet flux and remineralization depth in the Southern Ocean. Front. Mar. Sci. 6 https://doi.org/10.3389/fmars.2019.00230.

Longhurst, A.R., Bedo, A.W., Harrison, W.G., Head, E.J.H., Sameoto, D.D., 1990. Vertical flux of respiratory carbon by oceanic diel migrant biota. Deep Sea Research Part A. Oceanographic Research Papers 37, 685–694. https://doi.org/10.1016/0198-0149(90)90098-G.

Maas, A.E., Miccoli, A., Stamieszkin, K., Carlson, C.A., Steinberg, D.K., 2021. Allometry and the calculation of zooplankton metabolism in the subarctic Northeast Pacific Ocean. J. Plankton Res. 43, 413–427. https://doi.org/10.1093/plankt/fbab026.

Mackenzie, K.V., 1981. Nine-term equation for sound speed in the oceans. J. Acoust. Soc. Am. 70, 807–812. https://doi.org/10.1121/1.386920.

Maldonado, F., Packard, T.T., Gómez, M., 2012. Understanding tetrazolium reduction and the importance of substrates in measuring respiratory electron transport activity. J. Exp. Mar. Biol. Ecol. 434–435, 110–118. https://doi.org/10.1016/j.jembe.2012.08.010.

Manno, C., Stowasser, G., Enderlein, P., Fielding, S., Tarling, G.A., 2015. The contribution of zooplankton faecal pellets to deep-carbon transport in the Scotia Sea (Southern Ocean). Biogeosciences 12, 1955–1965. https://doi.org/10.5194/bg-12-1955-2015.

Manno, C., Stowasser, G., Fielding, S., Apeland, B., Tarling, G.A., 2022. Deep carbon export peaks are driven by different biological pathways during the extended Scotia Sea (Southern Ocean) bloom. Deep Sea Research (Part II. Topical Studies in Oceanography) 205. https://doi.org/10.1016/j.dsr2.2022.105183.

Mayor, D.J., Anderson, T.R., Irigoien, X., Harris, R., 2006. Feeding and reproduction of *Calanus finmarchicus* during non-bloom conditions in the Irminger Sea. J. Plankton Res. 28, 1167–1179. https://doi.org/10.1093/plankt/fbl047.

Mayor, D.J., Cook, K., Thornton, B., Walsham, P., Witte, U.F.M., Zuur, A.F., Anderson, T.R., 2011. Absorption efficiencies and basal turnover of C, N and fatty acids in a marine Calanoid copepod. Funct. Ecol. 25, 509–518. https://doi.org/10.1111/j.1365-2435.2010.01791.x.

Mayor, D.J., Gentleman, W.C., Anderson, T.R., 2020. Ocean carbon sequestration: particle fragmentation by copepods as a significant unrecognised factor? Bioessays 42, 2000149. https://doi.org/10.1002/bies.202000149.

Mayor, D.J., Sanders, R., Giering, S.L.C., Anderson, T.R., 2014. Microbial gardening in the ocean's twilight zone: detritivorous metazoans benefit from fragmenting, rather than ingesting, sinking detritus. Bioessays 36, 1132–1137. https://doi.org/10.1002/bies.201400100.

Mayzaud, P., Razouls, S., Errhif, A., Tirelli, V., Labat, J.P., 2002a. Feeding, respiration and egg production rates of copepods during austral spring in the Indian sector of the Antarctic Ocean: role of the zooplankton community in carbon transformation. Deep Sea Res. Oceanogr. Res. Pap. 49, 1027–1048. https://doi.org/10.1016/S0967-0637(02)00012-2.

Mayzaud, P., Tirelli, V., Errhif, A., Labat, J.P., Razouls, S., Perissinotto, R., 2002b. Carbon intake by zooplankton. Importance and role of zooplankton grazing in the Indian sector of the Southern Ocean. Deep Sea Res. Part II Top. Stud. Oceanogr. 49, 3169–3187. https://doi.org/10.1016/S0967-0645(02)00077-2.

Menden-Deuer, S., Lessard, E.J., 2000. Carbon to volume relationships for dinoflagellates, diatoms, and other protist plankton. Limnol. Oceanogr. 45, 569–579. https://doi.org/10.4319/lo.2000.45.3.0569.

Omand, M.M., Steinberg, D.K., Stamieszkin, K., 2021. Cloud shadows drive vertical migrations of deep-dwelling marine life. Proc. Natl. Acad. Sci. USA 118, e2022977118. https://doi.org/10.1073/pnas.2022977118.

Osma, N., Fernández-Urruzola, I., Gómez, M., Montesdeoca-Esponda, S., Packard, T.T., 2016a. Predicting in vivo oxygen consumption rate from ETS activity and bisubstrate enzyme kinetics in cultured marine zooplankton. Mar. Biol. 163, 146. https://doi.org/10.1007/s00227-016-2923-x.

Osma, N., Maldonado, F., Fernández-Urruzola, I., Packard, T.T., Gómez, M., 2016b. Variability of respiration and pyridine nucleotides concentration in oceanic zooplankton. J. Plankton Res. 38, 537–550. https://doi.org/10.1093/plankt/fbw001.

Owens, T.G., King, F.D., 1975. The measurement of respiratory electron-transport-system activity in marine zooplankton. Mar. Biol. 30, 27–36. https://doi.org/10.1007/BF00393750.

Packard, T.T., Christensen, J.P., 2004. Respiration and vertical carbon flux in the Gulf of Maine water column. J. Mar. Res. 62, 93–115. https://doi.org/10.1357/00222400460744636.

Packard, T.T., Devol, A.H., King, F.D., 1975. The effect of temperature on the respiratory electron transport system in marine plankton. Deep Sea Res. Oceanogr. Abstr. 22, 237–249. https://doi.org/10.1016/0011-7471(75)90029-7.

Pakhomov, E.A., Froneman, P.W., Wassmann, P., Ratkova, T., Arashkevich, E., 2002. Contribution of algal sinking and zooplankton grazing to downward flux in the Lazarev Sea (Southern Ocean) during the onset of phytoplankton bloom: a Lagrangian study. Mar. Ecol. Prog. Ser. 233, 73–88. https://doi.org/10.3354/meps233073.

Piatkowski, U., Rodhouse, P.G., White, M.G., Bone, D.G., Symon, C., 1994. Nekton community of the Scotia Sea as sampled by the RMT 25 during austral summer. Mar. Ecol. Prog. Ser. 112, 13–28. https://doi.org/10.3354/meps112013.

Platnick, S., Hubanks, P., Meyer, K., King, M.D., 2015. MODIS Atmosphere L3 Monthly Product (08_L3). NASA MODIS Adaptive Processing System. Goddard Space Flight Center.

Polimene, L., Sailley, S., Clark, D., Mitra, A., Allen, J.I., 2017. Biological or microbial carbon pump? The role of phytoplankton stoichiometry in ocean carbon sequestration. J. Plankton Res. 39, 180–186. https://doi.org/10.1093/plankt/fbw091.

Prosser, C.L., 1961. Oxygen: respiration and metabolism. In: Prosser, C.L., Brown, J.F.A. (Eds.), Comparative Animal Physiology. W.B. Saunders, Philadelphia, pp. 165–211.

Razouls, S., Du Réau, G., Guillot, P., Maison, J., Jeandel, C., 1998. Seasonal abundance of copepod assemblages and grazing pressure in the Kerguelen Island area (Southern Ocean). J. Plankton Res. 20, 1599–1614. https://doi.org/10.1093/plankt/20.8.1599.

Riley, J.S., Sanders, R., Marsay, C., Le Moigne, F.A.C., Achterberg, E.P., Poulton, A.J., 2012. The relative contribution of fast and slow sinking particles to ocean carbon export. Global Biogeochem. Cycles 26, GB1026. https://doi.org/10.1029/2011GB004085.

Sanders, R.J., Henson, S.A., Martin, A.P., Anderson, T.R., Bernardello, R., Enderlein, P., Fielding, S., et al., 2016. Controls over Ocean Mesopelagic interior carbon storage (COMICS): fieldwork, synthesis, and modeling efforts. Front. Mar. Sci. 3 https://doi.org/10.3389/fmars.2016.00136.

Sarthou, G., Vincent, D., Christaki, U., Obernosterer, I., Timmermans, K.R., Brussaard, C.P.D., 2008. The fate of biogenic iron during a phytoplankton bloom induced by natural fertilisation: impact of copepod grazing. Deep Sea Res. Part II Top. Stud. Oceanogr. 55, 734–751. https://doi.org/10.1016/j.dsr2.2007.12.033.

Siegel, V., 1987. Age and growth of Antarctic Euphausiacea (Crustacea) under natural conditions. Mar. Biol. 96, 483–495. https://doi.org/10.1007/BF00397966.

Siegel, V., 1992. Review of length-weight relationships for antarctic krill. SC-CAMLR Selected Scientific Papers 9, 145–155.

Steinberg, D.K., Carlson, C.A., Bates, N.R., Goldthwait, S.A., Madin, L.P., Michaels, A.F., 2000. Zooplankton vertical migration and the active transport of dissolved organic and inorganic carbon in the Sargasso Sea. Deep Sea Res. Oceanogr. Res. Pap. 47, 137–158. https://doi.org/10.1016/S0967-0637(99)00052-7.

Steinberg, D.K., Landry, M.R., 2017. Zooplankton and the ocean carbon cycle. Ann. Rev. Mar. Sci 9, 413–444. https://doi.org/10.1146/annurev-marine-010814-015924.

Steinberg, D.K., Van Mooy, B.A.S., Buesseler, K.O., Boyd, P.W., Kobari, T., Karl, D.M., 2008. Bacterial vs. zooplankton control of sinking particle flux in the ocean's twilight zone. Limnol. Oceanogr. 53, 1327–1338. https://doi.org/10.4319/lo.2008.53.4.1327.

Swadling, K.M., Gibson, J.A.E., Ritz, D.A., Nichols, P.D., Hughes, D.E., 1997. Grazing of phytoplankton by copepods in eastern Antarctic coastal waters. Mar. Biol. 128, 39–48. https://doi.org/10.1007/s002270050066.

Tarling, G.A., Johnson, M.L., 2006. Satiation gives krill that sinking feeling. Curr. Biol. 16, R83–R84. https://doi.org/10.1016/j.cub.2006.01.044.

Tarling, G.A., Thorpe, S.E., 2017. Oceanic swarms of Antarctic krill perform satiation sinking. Proc. Biol. Sci. 284, 20172015 https://doi.org/10.1098/rspb.2017.2015.

Tarling, G.A., Ward, P., Atkinson, A., Collins, M.A., Murphy, E.J., 2012. Discovery 2010: spatial and temporal variability in a dynamic polar ecosystem. Deep Sea Res. Part II Top. Stud. Oceanogr. 59–60, 1–13. https://doi.org/10.1016/j.dsr2.2011.10.001.

Turner, J.T., 2015. Zooplankton fecal pellets, marine snow, phytodetritus and the ocean's biological pump. Prog. Oceanogr. 130, 205–248. https://doi.org/10.1016/j.pocean.2014.08.005.

Ward, P., Atkinson, A., Tarling, G., 2012. Mesozooplankton community structure and variability in the Scotia Sea: a seasonal comparison. Deep Sea Res. Part II Top. Stud. Oceanogr. 59–60, 78–92. https://doi.org/10.1016/j.dsr2.2011.07.004.

Wiebe, P.H., Benfield, M.C., 2003. From the Hensen net toward four-dimensional biological oceanography. Prog. Oceanogr. 56, 7–136. https://doi.org/10.1016/S0079-6611(02)00140-4.

Yang, G., Han, Z., Pan, J., Zhou, K., Wang, Y., Li, C., 2019. Contribution of zooplankton faecal pellets to carbon transport of the mesopelagic layers in the polynya region of Prydz Bay, Antarctica. Estuarine. Coastal and Shelf Science 222, 139–146. https://doi.org/10.1016/j.ecss.2019.04.006.

Yebra, L., Herrera, I., Mercado, J.M., Cortés, D., Gómez-Jakobsen, F., Alonso, A., Sánchez, A., et al., 2018. Zooplankton production and carbon export flux in the western Alboran Sea gyre (SW Mediterranean). Prog. Oceanogr. 167, 64–77. https://doi.org/10.1016/j.pocean.2018.07.009.

Zøllner, E., Hoppe, H.G., Sommer, U., Jürgens, K., 2009. Effect of zooplankton-mediated trophic cascades on marine microbial food web components (bacteria, nanoflagellates, ciliates). Limnol. Oceanogr. 54, 262–275. https://doi.org/10.4319/lo.2009.54.1.0262.